Aircraft Cruise Phase Altitude Optimization Considering Contrail Avoidance

by

Hang Gao

B.S. Aerospace Engineering
Georgia Institute of Technology, 2011

SUMMITTED TO THE DEPARTMENT OF AERONAUTICS AND ASTRONAUTICS IN PARTIAL FULFILLMENT OF THE REQUIREMENTS FOR THE DEGREE OF

MASTER OF SCIENCE IN AEROPSACE ENGINEERING
AT THE
MASSACHUSETTS INSTITUTE OF TECHNOLOGY

SEPMTEMBER 2013

Signature of Author: _____
Department of Aeronautics and Astronautics
August 22, 2013

Certified by: _____
R. John Hansman
Professor of Aeronautics and Astronautics
Thesis Supervisor

Accepted by: _____
Eytan H. Modiano
Professor of Aeronautics and Astronautics
Chair, Graduate Program Committee

Aircraft Cruise Phase Altitude Optimization Considering Contrail Avoidance

by

Hang Gao

Submitted to the Department of Aeronautics and Astronautics
On August 22, 2013 in Partial Fulfillment of the
Requirements for the Degree of Master of Science in
Aerospace Engineering

Abstract

Contrails have been suggested as one of the main contributors to aviation-induced climate impact in recent years. To reduce the climate impact of contrails, mitigation policies such as taxation will be necessary in the future to incentivize jet aircraft operators to reduce contrail production. Contrails form in regions of the atmosphere with the right ambient conditions and they can be avoided by flying around these regions; this research investigates one such contrail avoidance strategy that uses flight level optimization to minimize contrail formation. A cruise phase flight profile system model was developed in this research that optimizes for environmental objectives such as contrails, CO_2, and NO_x, alongside traditional objectives such as fuelburn and flight time.

Using this system model and 11 different aircraft types on 12 weather days, a preliminary study was done to determine the price range of contrail taxation that would incentivize airlines to operationally avoid contrails. Result suggests a price range of 0.12$/NM to 1.13$/NM on contrail tax would effectively incentivize contrail avoidance. Furthermore, since operating costs differ depending on the type of aircraft, a single price on contrail tax may incentivize contrail avoidance on a small aircraft, but not larger ones. To account for this difference, a method of assigning contrail tax to different aircraft types is introduced using the aircraft maximum takeoff weight.

Assuming airlines are incentivized to fly contrail avoidance strategies, the climate impact of the flight profiles was evaluated for 287 flights along 12 O-D pairs for the 24 hour day of April 12, 2010. Under various assumptions of contrail radiative forcing and time horizon of climate impact evaluation, the flight level optimization reduced the average climate impact per flight by as much as 39.1% from a baseline of wind-optimal flight at optimal cruise altitude. In comparison, a complementary lateral optimization method reduced 13.3% from the same baseline. Furthermore, flight level optimization shows to be more fuel efficient by reducing the climate impact of contrails by as much as 94% from the baseline, compared to 60% using the lateral approach. In terms of the CO_2 emission from the additional fuelburn, the climate impact of lateral method was 4 times higher than the flight level approach. Lastly, result shows that designing for long-term environmental objectives is more energy efficient (reduction in climate impact per additional kilogram of fuel used) than short-term, which suggest reducing CO_2 emission is favored over contrail avoidance in designing for climate impact optimal flight profiles.

Thesis Supervisor: R. John Hansman

Title: Professor of Aeronautics and Astronautics

Table of Content

Chapter 1 – Introduction 9

1.1 Motivation 9

1.2 Research Goals 12

1.3 Overview 12

Chapter 2 - Background 15

2.1 The Physics of Contrails 15

2.2 Climate Impact Metric 19

2.3 Climate Impact of Aviation 20

2.4 Climate Impact of Contrails 21

2.5 Prospect of Contrail Mitigation Policy 22

2.6 Advancement in Mitigation Approaches: 23

2.6.1 Technological Approaches: 23

2.6.2 Operational Approaches: 24

2.7 Current Operations 25

2.8 Incorporation of Environmental Impact Objectives 26

2.9 Tradeoff Analysis Framework 27

2.9.1 Valuation (λ-set) 28

Chapter 3 - Methodology 31

3.1 Tradeoff Framework with Optimization 31

3.2 Data Sources 33

3.2.1 Weather Data 33

3.2.2 Contrail modeling: 35

3.2.3 Aircraft performance modeling: 36

3.3 System model 38

3.3.1 Defining the Cruise Profile 39

3.3.2 Vertical Optimizer Heuristic 40

3.3.3 Weight Convergence 41

3.4 Study-specific System Models 42

3.4.1 Cost-based Optimization 42

3.4.2 AGTP-based optimization 43

3.4.3 Illustration of the system model solutions 45
3.5 Preliminary Study 47
Chapter 4 – Contrail Tax Impact Study 51
4.1 Weather Sensitivity 51
4.2 Aircraft Sensitivity 55
4.3 Price Cap 57
4.4 Fuelburn Tradeoff 60
4.5 Summary of Contrail Tax Impact Study 61
Chapter 5 – Climate Impact Study 63
5.1 Impact of Flight Level Optimization 64
5.2 Fuel Efficiency Comparison 67
5.3 Energy Efficiency of Climate Optimal Strategies 70
5.4 Summary of Climate Impact Study 71
Chapter 6 - Conclusion 73
6.1 Contrail Tax 73
6.2 Climate Impact 74
Bibliography 76
Appendix A 78
Appendix B 79
Appendix C 80
Appendix D 81

List of Figures

Figure 1 The latest estimation of aviation radiative forcing 10
Figure 2 Contrail coverage for the year 2002 11
Figure 3 Non-persistent contrail formation 17
Figure 4 Persistent contrail formation 17
Figure 5 Various estimates of the aviation RF for 1992 and 2000 21
Figure 6 Tradeoff framework 27
Figure 7 Tradeoff framework with optimization 32
Figure 8 Representative weather using RUC data 34
Figure 9 Weather interpolation 36
Figure 10 The system model 38
Figure 11 Visualization of the graph network of a cruise profile 39
Figure 12 The runtime of each additional solution using KSP 41
Figure 13 The cost-based system model. 42
Figure 14 The AGTP-based system model 44
Figure 15 Contrail RF and time horizon in the system model 44
Figure 16 Representative flight profile from LAX to JFK 45
Figure 17 The same representative flight, here using the AGTP-based optimizer 46
Figure 18 3-D visualization of the 5 tradeoff variable components using PCA 48
Figure 19 Variable correlation using PCA 49
Figure 20 Weather days for LAX-JFK for the first day of every month of 2009 52
Figure 21 Example flight profile 53
Figure 22 Sensitivity of contrail avoidance to weather conditions 54
Figure 23 Contrail production cost tradeoff 55
Figure 24 The mean distance of contrail produced 56
Figure 25 The rate of contrail avoidance per additional $/NM 57
Figure 26 Normalized sensitivity plot 59
Figure 27 Cost tradeoff 60
Figure 28 Fuelburn tradeoff points 61
Figure 29 Representative lateral track types for LAX-JFK 65
Figure 30 Vertical AGTP optimization. 66
Figure 31 The average net AGTP reduction of various operational strategies 66
Figure 32 Comparison between the climate impact reduction and fuel efficiency 68
Figure 33 Plot of climate impact and fuel efficiency 69
Figure 34 Sensitivity of AGTP at different contrail RF assumptions 70
Figure 35 The energy efficiency 71
Figure 36 Clusters of 2/1/2009 LAX-JFK flight profile solution space 78
Figure 37 All flight profiles in the tradeoff solution space 78
Figure 38 The reduction of average climate impact 79
Figure 39 The energy efficiency of climate impact optimal strategies 81

List of Tables

Table 1 NARR-A and RUC 20km **35**
Table 2 All aircraft types used ordered by MTOW **37**
Table 3 Climb descent coefficients **40**
Table 4 Current value structure **43**
Table 5 The AGTP of fuelburn **45**
Table 6 Variable component angle from PCA. **49**
Table 7 Derived price cap for 11 aircraft types **59**
Table 8 The 12 city pairs **64**
Table 9 AGTP reduction of strategies **80**

Chapter 1 – Introduction

This section motivates the growing climate impact of contrails and the need for mitigation policies to incentivize aircraft operators to fly contrail avoiding trajectories. The objectives of this thesis are to answer the open questions that arise from these motivations.

1.1 Motivation

Contrails, or aviation-induced cirrus clouds, are not traditionally recognized as a major contributor to aviation-induced climate impact as compared to CO_2, NO_x, and other particulate emissions. However recent research efforts in Europe have verified the global warming contribution of contrails; one study suggest that contrails and contrail-induced cirrus are the largest single climate impact component from aviation, more than that of CO_2 emissions (Burkhardt & Karcher, 2011). While uncertainty still remains in quantifying the climate impact of contrails, its significance has been suggested across a number of studies. In the latest estimate, climate impact contribution of contrails and contrail-induced cirrus clouds is comparable to that of CO_2 and NO_x emissions (Figure 1).

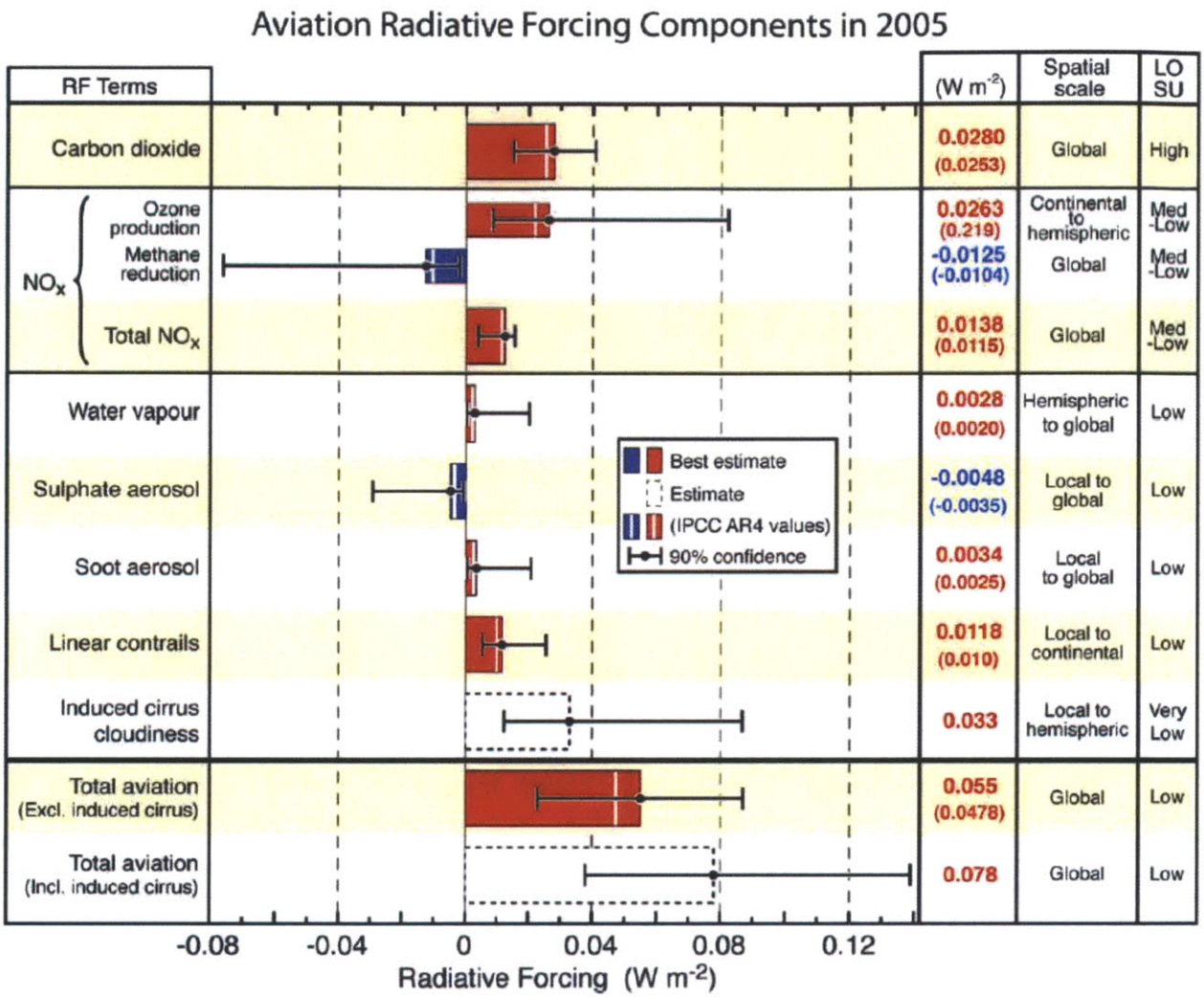

Figure 1 The latest estimation of aviation radiative forcing (a measure of climate impact) in 2005 by Sausen et al. The main RF components are CO_2, NO_x, and contrails (linear and induced cirrus cloudiness). (Sausen, 2005)

Contrails include linear contrails and the contrail-induced cirrus cloudiness; contrails can grow from the initial line-shaped cloud and spread in coverage given the right weather conditions. In fact, contrail coverage reached up to 8-10% of the airspace in heavy air traffic regions such as the northeast United States and central Europe during the year 2002 (Figure 2). Alongside the growth of the global passenger and freighter jet aircraft fleet, which is projected to double from 2011 to 2031, global contrail coverage will continue to grow unless a mitigation policy such as taxation on contrail production is implemented. Such a policy intends to internalize the social cost of contrails by putting a price on contrail production.

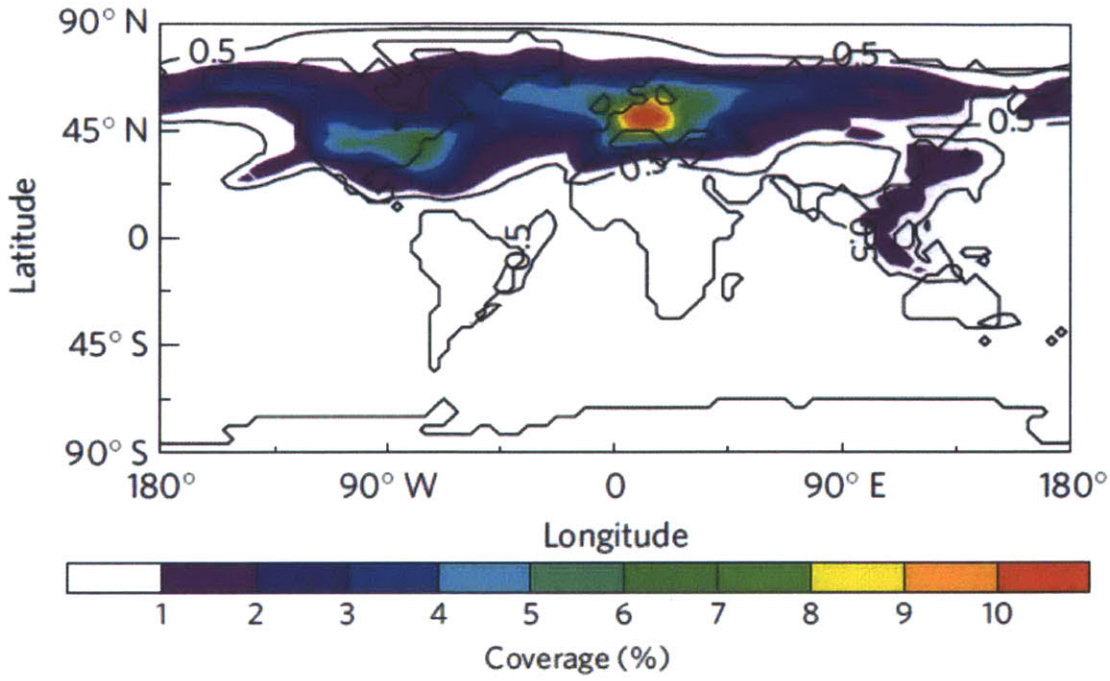

Figure 2 Contrail coverage for the year 2002 using a module developed using ECHAM4, an existing climate model developed by IPCC. The results were successfully verified using satellite observations. (Burkhardt & Karcher, 2011)

Once a policy is established, jet aircraft operators will be incentivized, from a cost perspective, to minimize contrail production during operations. One such contrail minimizing strategy is to operationally avoid contrail producing regions of the airspace by way of cruise phase flight level optimization.

In light of all this, some open questions arise which this thesis will attempt to answer: How, and at what price range, would contrail tax impact cruise operations? And once contrail tax incentivizes operators to fly contrail avoidance strategies, what would be the climate impact of these strategies? There exist other operational strategies that use lateral maneuvering for contrail avoidance, how does the flight level optimization strategy compare? Is one strategy more fuel efficient than the other? Should the optimal strategies be designed for short-term or long-term climate impact? Due to the uncertainty in the current estimate of the climate impact of contrails, how sensitive are the contrail avoidance strategies to different estimates?

1.2 Research Goals

This research attempts to accomplish two main goals:

1. Gain an understanding of the impact of contrail tax on the choice of the optimal flight profile and establish a contrail tax price range which contrail avoidance strategy is operationally cost-effective.
2. Evaluate the effectiveness of the flight level optimization strategy in minimizing climate impact.

1.3 Overview

The objectives of this research center on the two main research goals and they are evaluated using two studies: Contrail tax impact study and climate impact study. In order to tackle these objectives, a cruise phase flight level optimization tool was developed to compute contrail avoidance strategies by enabling tradeoffs between contrail production, fuel consumption, flight time, and CO_2 and NO_x emissions. By adjusting flight levels along the flight path, the optimal profile is found by minimizing either the total trip cost (in U.S. dollar) or climate impact (in AGTP, a climate impact metric) for the contrail tax impact study and the climate impact study, respectively. From the two main research goals, a number of objectives arise as summarized below:

Contrail Tax Impact Study

- To understand how contrail avoidance may vary based on the weather and aircraft type flown, sensitivity analyses will be done for different weather conditions and different aircraft types.
- To investigates how contrail tax will impact the choice of the optimal flight profile. Using the cost-based optimizer, the optimal profile is found by trading off between the costs of fuel burn, flight time, CO_2 emission, NO_x emission, and contrail production, where the cost of contrail production alludes to the contrail tax. This study will determine a price range of contrail taxation at which contrail avoidance strategy is cost-effective.

Climate Impact Study

- This study uses the climate impact optimizer to investigate the effectiveness of the flight level optimization strategy in minimizing climate impact. The optimal profile is found by trades off between the climate impact of contrail production and CO_2 emission. Since flight level optimization can be implemented on a variety of different lateral routes such as the great circle route and wind-optimal route, their climate impact will also be examined.
- There are two operational approaches to avoid contrail forming regions: flight level changes and lateral deviations. Complementary to the flight level optimization strategy developed in this research, a research team at NASA Ames has developed a lateral route optimization strategy. The objective is to compare the contrail mitigation and fuel consumption characteristics of both strategies.
- Climate impact is measured at the end of a specific time horizon (i.e. 25, 50, 100 years) therefore the design of the climate impact optimal strategy differs depending on this time horizon. Using the energy efficiency metric, strategies designed for different time horizons are flown and their efficiency are evaluated.
- Due to the uncertainty in estimating the climate impact of contrails, this study uses a range of contrail impact values to evaluate the sensitivity of the results.

Chapter 2 - Background

This section discusses the physics behind contrails, along with current best estimates of its climate impact using radiative forcing (RF) as the metric. Using RF as a metric, the climate impact of contrails is compared relative to all known aviation-induced emissions. Once the significance of contrails is establish, the current state of research in contrail avoidance strategies will be summarized. One promising strategy is to operationally avoid contrail forming regions of the airspace by adjust the flight level of the aircraft. To implement this strategy, contrail production will be integrated as an additional constraint in the planning of aircraft cruise operations. The last portion of this chapter will detail the framework by which contrail avoidance is incorporated into the cruise phase route optimization problem.

2.1 The Physics of Contrails

Contrails are clouds of ice particles formed by the condensation of aircraft engine exhaust byproducts such as soot emissions and water vapor, often assisted by the decreased pressure in the ambient air caused by the wingtip vortices (Schrader, 1997). More specifically, the engine exhaust injects water vapor, sulfates, hydrocarbons, and soot particulates into a cold ambient environment where the air is saturated with respect to water, thus forming water droplets that

freeze due to the low temperature. These induced cirrus clouds may further persist if the air is supersaturated with respect to ice. Interestingly, natural cirrus formation requires that the ambient air to be of higher ice supersaturation conditions than that of these contrail-induced cirrus clouds. It is thus inferable that there exist cloud-free regions of the airspace where only contrail, not natural, cirrus may form (Burkhardt & Karcher, 2011).

Contrails are the result of the mixing between warm unsaturated engine exhaust gases and cold water-saturated ambient air. The trail of warm exhaust gases drops in temperature and pressure as it approaches ambient conditions. When the ambient air is saturated with respect to water, the water droplets will freeze due to the low temperature. The criterion for saturation with respect to water is met when the relative humidity with respect to water, RH_w, is greater than a critical value. The critical relative humidity of the ambient air, r_{crit}, is a function of the saturation vapor pressure over water, e_{sat}^{liq}, at a given temperature, T, greater than a critical temperature of contrail formation, T_{crit}.

$$r_{crit} = \frac{G(T - T_{crit}) + e_{sat}^{liq}(T_{crit})}{e_{sat}^{liq}(T)}$$

T_{crit} can be derived and implemented as a constraint in finding contrail producing regions as follows:

$$T_{crit} = -46.46 + 9.43\ln(G - 0.053) + 0.72\ln^2(G - 0.053)$$

Where $G = \frac{EI_{H_2O}C_P P}{\varepsilon Q(1-\eta)}$, EI is the emission index, C_P is the isobaric heat capacity of air, P is the ambient air pressure, ε is the ratio of molecular masses of water and dry air, Q is the specific combustion heat, and η is the average propulsion efficiency of the jet engine (Alduchov & Eskridge, 1996).

In addition to finding regions with atmospheric conditions that allow contrail formation, the ice cloud may or may not persist depending on the saturation of the ambient air with respect to ice. If the air is not saturated with respect to ice, $RH_i < 1$, the ice crystals will eventually sublimate back into the ambient air as water vapor (Figure 3). Since the humidity (mass of water vapor per unit volume of air, which is proportional to pressure) of the trail of gases is directly

proportional to the temperature, the lifetime of the contrail can be depicted as a line against the phase diagram of water.

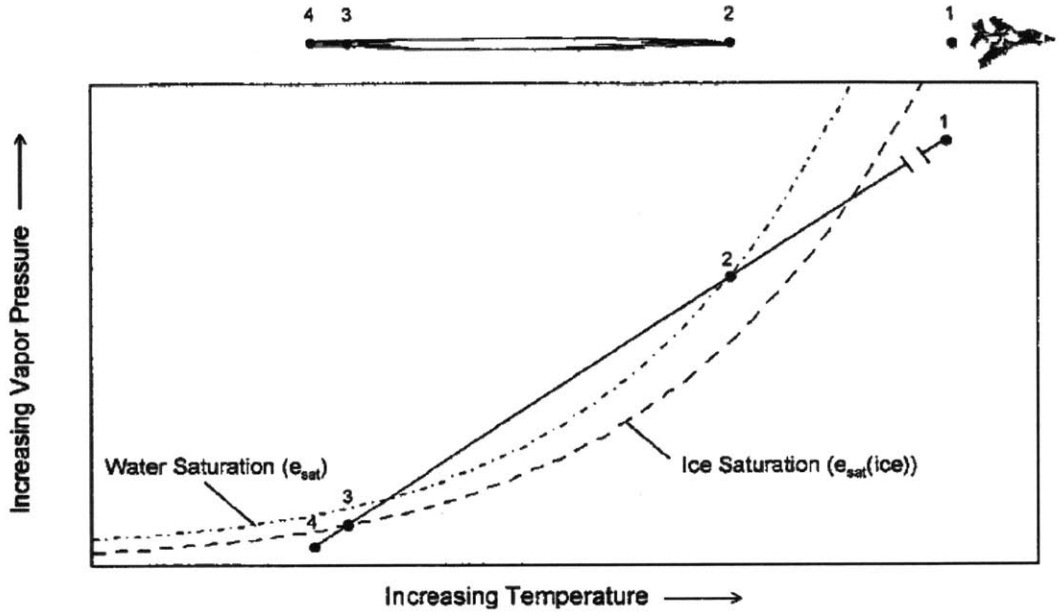

Figure 3 Non-persistent contrail formation due to the ambient air condition below ice saturation. From state (3) to (4) of the ice crystals that make up the contrail sublimates back into the ambient air, therefore not persisting (Schrader, 1997).

If the relative humidity with respect to ice, RH_i, is greater than 100%, then the contrail will persist for a longer period of time before it sublimates.

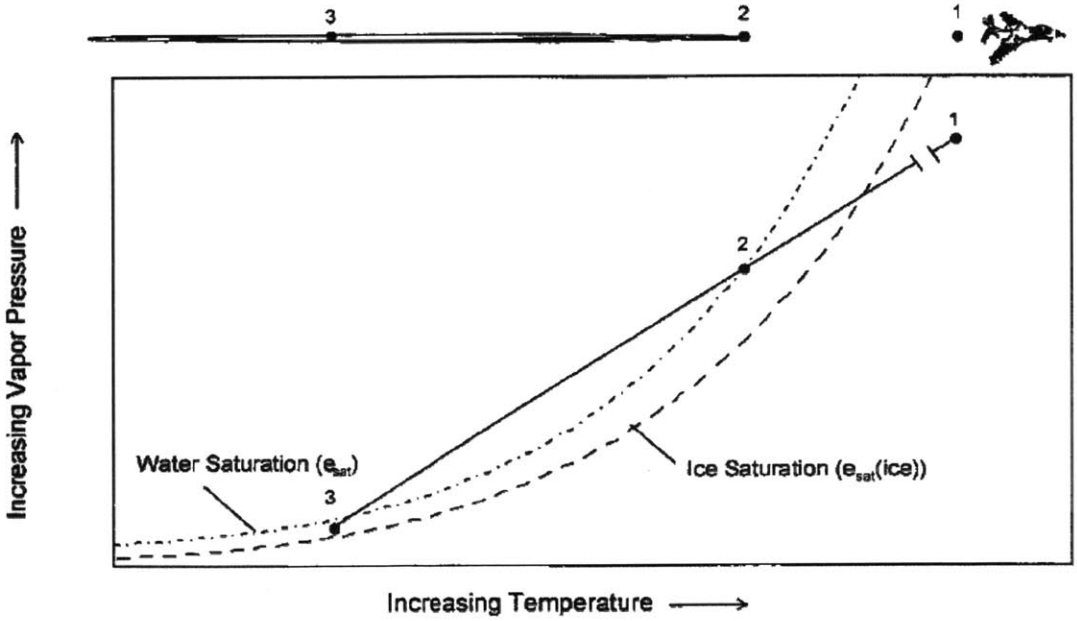

Figure 4 Persistent contrail formation occurs when the ambient air is supersaturated with respect to ice. The phase of the ice crystals that make up the contrail region remain in state (3), thus persists

The RH_i is found using the ratio between the saturation vapor pressure over water and ice, which has been shown to give results accurate to less than 1% of the standard humidity data (Alduchov & Eskridge, 1996).

$$RH_i = RH_w * \frac{6.0612e^{18.102 \cdot T/(249.52+T)}}{6.1162e^{22.577 \cdot T/(273.78+T)}}$$

Contrails not only persist, but also grow. Satellite observations have shown significant increase in cirrus cloud coverage over airspace with heavy air traffic. While contrails are initially line-shaped clouds trailing the aircraft, due to wind-shear they may directly transform into cirrus clouds given favorable meteorological conditions. In fact these clouds have shown lifetimes upwards of 17 hours based on satellite observations and can cover up to ten times the coverage of the initial linear contrail (Sausen, 2005). Contrail formation rates have been measured to upwards of 140 m/min horizontally and 18 m/min vertically (Jager, Freudenthaler, & Homburg, 1998), making them geometrically greater in width than height. Another mechanism by which these anthropogenic clouds may form does not require an initial contrail. The indirect effect of aviation soot emissions on cirrus in the absence of contrails depend on the concentration of and interaction between the emission particles and the ambient air. Essentially, the aerosol injected into the air may act as ice nuclei that seed the formation of cirrus clouds at the right mixing conditions. Albeit there is an inherent uncertainty in distinguishing them from naturally formed cirrus clouds that exist in these satellite observations, thus further meteorological studies are being conducted to refine these results.

The climate impact of contrails is attributed to the radiative trapping of the contrail clouds. In contrast to other emissions such as carbon dioxide gas that mainly absorbs the longwave energy radiating from the Earth's surface back out into space, contrails has an additional effect of reflecting the downward shortwave energy from the Sun during the daytime, which is commonly known as albedo cooling. Climate impact is measured by quantifying the net energy radiating in and out of the Earth's atmosphere. The following section will detail one way climate impact can be quantified.

2.2 Climate Impact Metric

Before looking at the climate impact of contrails, it is important to first understand the metric used in measuring climate impact. A widely used method of measuring the impact of human and natural factors on climate uses the concept of radiative forcing (RF). Definitively, radiative forcing measures the perturbation of the Earth's energy budget between two time periods (typically referenced to year 1750, which marks the beginning of the Industrial Era) by finding the net energy difference measured at the tropopause (i.e. FL360 for mid-latitude regions) between the radiative energy from the Sun and the radiated energy from Earth's surface albedo. RF is measured in the unit of watts per square meter [Wm^{-2}]. The incoming energy the Sun is positive RF and the outgoing energy is designated as negative RF. The RF concept is used to assess the contribution of various environmental factors that affect the radiative balance of Earth; the net positive RF effect of trapping outgoing longwave radiation is commonly known as the greenhouse effect. The standard method of measuring climate impact uses the concept of RF to quantify a metric called global-warming potential (GWP). Most notably used in the international treaty on emissions control known as Kyoto Protocol, GWP is the time integral of the radiative forcing, $\Delta RF(t)$, over a region for a specific time interval T_0 to T_1.

$$GWP(T_1) = \int_{T_0}^{T_1} \Delta RF(t)dt$$

Intuitively, this is the net amount of energy trapped by the emission species being measured for a specific time interval. GWP is often used in reports as referenced to an equivalent amount of CO_2 needed to generate the same forcing, as is the case for the Kyoto Protocol. This method of quantifying climate impact is relatively easy to implement; the IPCC First Assessment Report (FAR) described GWP as a "simple approach" for measuring climate impact. However, using GWP also has a few disadvantages (Peters, 2011). Most notably, GWP is a time-integrated measurement that would not distinguish a gas with low RF and long lifetime from another gas with a high RF with a short lifetime. To overcome some of the disadvantages, a novel climate impact metric was developed to take advantage of RF's approximately linear relationship to the change to the global mean surface temperature. This concept is formally known as the Absolute Global Temperature Change Potential (AGTP):

$$AGTP(T_1) = \int_{T_0}^{T_1} \delta(T_1 - t) * \Delta RF(t) dt$$

AGTP is found using a convolution integral between the time interval between T_0 and T_1, where $\delta(T_1\text{-}t)$ is the impulse response function for the surface temperature change at T_1 due to a radiative forcing $\Delta RF(t)$ applied at time t. The derivation from the RF to the surface temperature change is based on a first-order climate model that assumes exponential decay in the RF. The exponential decay of $\Delta RF(t)$ reflects the lifetime of an emissions species via a parameter that captures the heat capacity and climate sensitivity of the gas. Using AGTP, the resulting value is in the unit of kelvin and the decay parameter reflects the residual gas lifetime. Depending on the time horizon, which denotes the time interval from T_0 to T_1, of interest, the AGTP metric captures the decay characteristic of the RF contributed by each gas. For contrails, the AGTP contribution drops off significantly for longer time horizons. In contrast, CO_2 gas are resident in the upper atmosphere for much longer periods of time and thus their AGTP contribution diminishes less drastically. This behavior is captured in the climate impact study, where contrail avoidance strategies are optimized based on an AGTP-minimal objective function. The AGTP contribution from contrails and CO_2 emission are evaluated for a range of time horizons: 25, 50, and 100 years.

2.3 Climate Impact of Aviation

Before diving into a discussion on the climate impact of contrails, let's first put climate impact of aviation into perspective. Compared to the total anthropogenic RF, aviation contributed 3.5% in 1992, and is projected to increase to 5% by 2015 (IPCC, 2012). The impact of aviation emission is unlike other types of emission in that the injections are made directly into the upper troposphere and lower stratosphere (at the ozone layer) where they are most potent. The main components of climate impact due to aviation include carbon dioxide (CO_2), nitrogen oxides (NO_x), water vapor (H_2O), sulphate (SO_x), soot, and contrails. Of these emissions, CO_2, NO_x, and contrails are the biggest contributors (Figure 1). Unlike CO_2 that has a decadal lifespan allowing for complete mixture into the atmosphere, other gases such as NO_x, SO_x, and water vapor (contrail precursor) exist for a shorter period of time and are more concentrated near the flight path where they were injected. Due to these temporal and local characteristics, these gases cause more short-term regional climate responses as opposed to long-term global ones

characteristic of CO_2.While the impact of common climate impact gases such as CO_2 and NO_x are fairly well understood with an established history of assessments followed by policy and taxation proposals, contrails is relatively less understood within the aviation community and have yet to generated enough interest to initiate any efforts to formulate a mitigation policy.

2.4 Climate Impact of Contrails

The RF estimates of linear contrails, excluding contrail-induced cirrus clouds, have varied throughout the years with large uncertainty. Beginning in 1999, the first assessment was conducted by the IPCC on the climate impact of aviation for the years 1992 and 2000 using RF. Recalling that the RF for a particular year represents the energy budget perturbation compared to the 1750 baseline, the RF due to linear contrails in 1992 was modeled to be $20mWm^{-2}$ and was projected to increase to $34mWm^{-2}$ by 2000 (Figure 5), which signifies a $14mWm^{-2}$ increase.

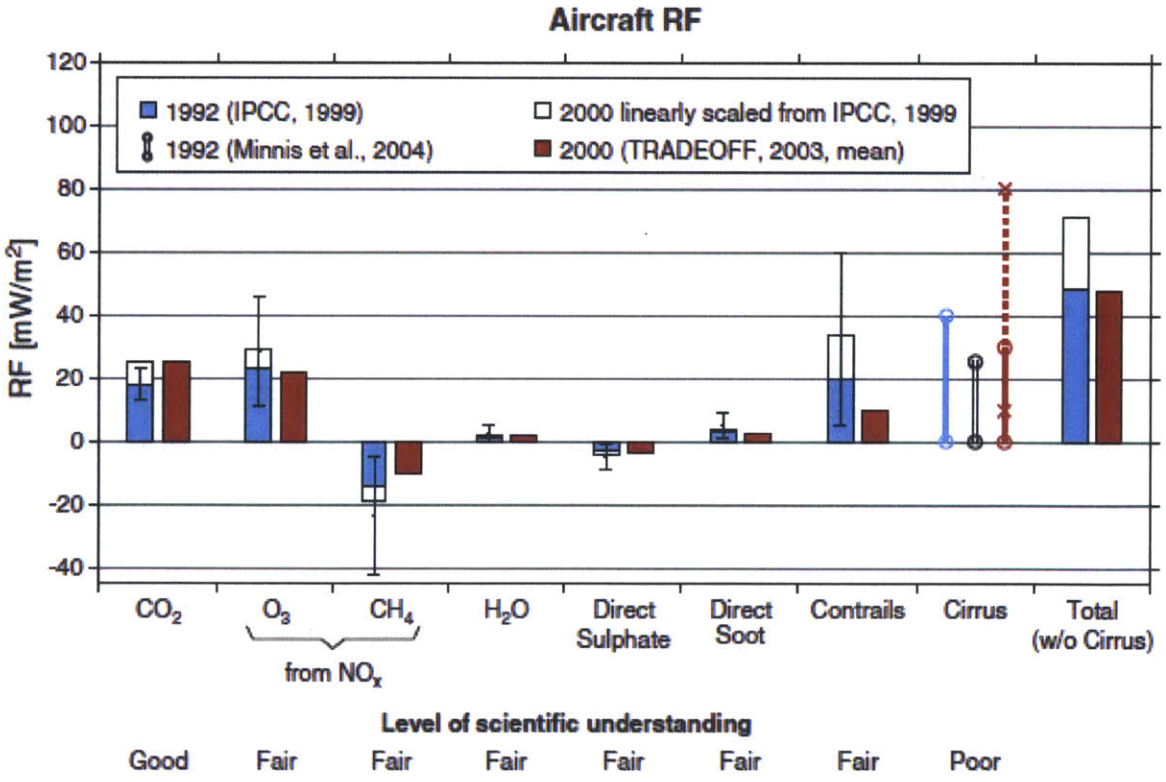

Figure 5 Various estimates of the aviation RF for 1992 and 2000 throughout the years by IPCC and Sausen. Note the variation in the estimate of contrail RF, ranging from 10 to 30 mWm^{-2}.

In 2005, a European research effort (2000-2003) published new estimates of the RF for the year 2000 using more refined contrail coverage and microphysical property modeling. The improved estimate cuts the old value by a factor of three to $10mWm^{-2}$ (Sausen, 2005). In the

latest estimates on the contrail RF of year 2005 found a comparable value of 11.8mWm^{-2}. Therefore although the uncertainty still remains in estimates of contrail RF, independent studies have recently converged on a smaller range of values. Due to the uncertainty in contrail RF estimates, a range of RF values were used in this thesis: 3.3, 10, and 30mWm^{-2}.

The RF estimates given above focused only on the linear contrails trailing after the aircraft, but neglects the contrail-induced cirrus clouds that appear hours after the contrail formation. The latest research that tries to model the whole life cycle of contrails, including the induced cirrus, suggest that the RF contribution from the subsequent cirrus clouds are almost ten times in coverage than that of the initial linear contrails; albeit the induced cirrus clouds generally have a decayed RF. The conclusion from these studies suggests that the contrails, despite their short lifetime, have a great radiative impact at any one time due to their high RF, resulting in climate impact comparable to that of CO_2 emissions (Burkhardt & Karcher, 2011). An important point to distinguish here is the difference in the lifetimes of contrails and carbon dioxide; assuming all the aircraft in the world are grounded indefinitely, the climate impact due to carbon dioxide will continue to last but the impact of contrails will cease due to their short lifetime. However, at the rate that the air transportation system is currently growing, the impact of contrails will be hard to overlook.

2.5 Contrail Mitigation Policy

As are often done with other climate impact emissions, mitigation policies will likely arise to set limitations on contrail production; it may be requiring jet aircraft operators to internalize the social cost through taxation or setting up a cap and trade system between operating entities, namely airlines. Contrail production, like other greenhouse gas emissions, is a negative externality (unaccounted adverse impact on society) that should be associated with a social cost in the near future if the implications from the recent climate impact studies remain true. A pigouvian tax is a method to internalize the negative externality and is often used for emissions tax. It is foreseeable an implementation of pigouvian tax on contrail production will be placed on airlines, which may be an effective method of mitigate the climate impact of contrail formations. While the social cost per unit (distance or time) of contrail remains to be estimated, it becomes interesting to ask how contrail tax may impact current aircraft operations relative to the current cost structure (current jet fuel price, block hour operating cost, emissions social costs).

As such, the implication of the contrail tax impact study is to give a preliminary idea of the marginal operating cost of contrail avoidance. Under the hypothetical scenario such policy creates, aircraft operators will become incentivized to reduce contrail production through mitigation approaches.

2.6 Mitigation Approaches

There are a variety of approaches to minimize contrail production. From a technological standpoint contrail production can be reduced by implementing new engine concepts and aircraft design, alternative fuel and combustion processes, and dedicated prevention devices. Operationally, contrail production can be minimized by using temporal and spatial avoidance strategies.

2.6.1 Technological Approaches

For contrail formation, the mixing process of the engine exhaust with the ambient air is dictated by, among other variables, the engine efficiency. At lower altitudes, more efficient engines cause an increase in contrail producing regions due to their cooler exhaust and more water content. However, at higher altitudes, the difference diminishes (Noppel, 2007). In terms of modifying the microphysics of the exhaust particles, filtration technology during or post combustion can help to reduce the RF of contrails produced. Aircraft design improvements primarily focus on lowering the optimal flight altitude, where contrails are less likely to form. Modification to the wing design may help to minimize wind vortices that assist in exhaust mixing. Fuel-based improvement options such as reducing sulfur content, fuel additives, or fuel alternatives (hydrogen) will lower water vapor output, but at a price of larger exhaust particles that will remain in the atmosphere to seed contrails, albeit lower RF contrails.

Some of these technological approaches are sound in theory. However, recognizing that technological turnover rate of aviation is driven by the rate at which the global fleet evolves via retrofitting and purchasing new aircraft, added with the fact that the average utilization lifetime of an aircraft is on the order of 25 years, the impact of technological advancements is rather slow. Additionally, most of these technological improvements can, at best, suppress the net RF of contrails produced, not eliminating them.

2.6.2 Operational Approaches

Operational changes to minimize contrail production take advantage of the temporal and spatial characteristics of contrails. For example, the RF of contrail is higher in the evening since shielding effects during the day reduces daytime RF. During the day contrails are able to deflect short-wave radiative energy from the Sun, thus decreasing the positive RF component. Therefore from a purely contrail minimizing perspective, it would be strategic to limit flights in the evening. To show the shielding effect of contrails during the daytime, the mean net global radiative forcing at the top of the troposphere (12 km or roughly FL390) during daytime has been modeled to be less than that of the full day (R. Meerkotter, 1999). Furthermore, contrail RF has been found to be less during sunrise and sunset (high solar zenith angles) than other times of the day (Myhre & Stordal, 2001), which seem to suggest more flights should be scheduled at dawn and dusk. However, limiting flights to certain times of the day is operationally undesirable given the capacity and economic disadvantages.

Spatially constrained strategies can also be formulated to minimize the net RF impact of the contrail formation. One method is to flying through regions that maximizes the contrail's radiative shielding component (negative RF) while minimizing trapping reflected radiative energy (positive RF). This method takes advantage of the fact that Earth's surface has regions of high and low surface albedo (reflectivity). For example, snow-covered regions have high albedo due to high reflectivity of the white surface. Therefore, it is preferable to fly over low albedo regions to minimize the positive RF component. In the extreme case, according to IPCC, scenarios involving cold surfaces, low surface albedo, and high atmospheric humidity may result in net cooling (net negative RF) due to contrails ((IPCC), 1999). Although sound in theory, the unpredictable nature of contrail spreading deems this approach less effective. While the aircraft may strategically fly over low albedo areas, the contrails formed are likely to drift and grow into surrounding areas of higher albedo.

Another approach is to execute flight plans that are designed to minimize flying through contrail producing regions, which can be done by incorporating contrail production as an additional variable to the route optimization problem. Contrail avoidance can be achieved by either lateral deviations or vertical flight level changes, which is the strategy used in this research. While vertical contrail avoidance may require less deviation than lateral, operationally, the

additional flight level changes may introduce undesirable complexity in the airspace for the pilot and the controller, not to mention passenger inconvenience. Operational strategies with contrail mitigation have been proposed in the past and route optimization methods have been developed from a number of studies. However, until recently none of the methods considered wind in their simulation environment i.e. (Gierens, 2008) & (Campbell, 2008). By omitting wind effects from the route optimization problem, potential fuel efficient solutions are lost, making the results unrealistic. Recent efforts, mainly conducted by a research group at NASA Ames Research Center, have used actual weather forecast and air traffic data i.e. (Sridhar B. C., 2011) and (Sridhar, 2012). At NASA Ames, the route optimization is done via horizontal maneuvers and does not allow for flight level changes, which is complementary to the approach taken in this thesis. An interesting question to ask is whether lateral or vertical (flight level) optimization is more effective as a contrail avoidance strategy. To answer this question, part of the climate impact study is in collaboration with the NASA Ames research team as the two approaches are compared in terms of their effectiveness in climate impact mitigation and fuel efficiency. The incorporation of contrails to the route optimization problem means increasing the tradeoff dimensions of the flight planning method of current aircraft operations. So before discussing the incorporation of contrail and other environmental objectives into the current flight planning method, the following section will give a background of the method commonly used by airlines today, the cost index (CI).

2.7 Current Operations

In today's operations, the optimization method that most airlines implement in their flight management computer (FMC) uses the cost index (CI) concept. CI is a parameter that reflects the relative importance between the trip block flight time and the trip fuel consumption.

$$CI = \frac{Operating\ Cost\ [\frac{\$}{Bhr}]}{Fuelburn\ Cost\ [\frac{¢}{lb}]}$$

This index is the ratio of the operating cost (minus fuel) in dollars per block hour and fuelburn cost in cents per pound of fuel. By taking the desirable CI submitted by the operator, the FMC will back out the corresponding performance parameters to calculate the most appropriate

speed from climb to descent (Roberson, 2007). To give some intuition on the range of possible CI values for cruise operations, zero results in the most fuel efficient flight plan and maximum CI results in the fastest flight plan. It is clear from this approach that only fuel consumption and operating cost are considered in finding the optimal flight plan, making this a two-dimensional optimization problem. By incorporation environmental objectives such as contrails and other emissions to the function, the dimension of the optimization problem increases to a highly dimensional tradeoff problem. High dimensionality is one of a number of challenges posed by the considering of environmental objectives into the optimization problem.

2.8 Incorporation of Environmental Impact Objectives

To increase the scope of the trajectory optimization problem to include environmental objectives such as contrails, CO_2, and NO_x, a number of issues must be addressed.

1) Highly dimensional tradeoff problem: The incorporation of CO_2, NO_x, and contrails along with the traditional performance objectives of fuel consumption and block operating time calls for an optimization technique capable of handling a tradeoff hyperspace with a large number of possibly intercorrelated objective variables.
2) Multiple metrics: The traditional performance objectives are typically measured in dollar cost per gallon of fuel or block operating hour. On the other hand, environmental objectives are measured by climate impact metrics such as AGTP. Therefore the joint optimization problem must be capable of cross-metric evaluations that make intuitive sense.
3) Multiple stakeholders: Typical of most air transportation system design and optimization problems, the cruise operations problem is of interest to a number of different stakeholders in the aviation community. The airlines are interested in cost efficiency and customer satisfaction, the air traffic control towers are interested in safety, capacity, and workload, and the environment interest groups are interested in climate impact of aviation.

In light of these requirements inherent to the optimization problem, this study looks to utilize a suitable tradeoff framework that has been developed previously for these purposes.

2.9 Tradeoff Analysis Framework

The framework was designed for the purpose of analyzing tradeoff hyperspaces often seeing in the design and operations of systems that consider a high number of tradeoff variables (O'Neill & Hansman, 2012). The robustness of the framework allows it to handle a wide range of highly dimensional tradeoff problems that exist in the air transportation system, making it appropriate for the cruise operations optimization that considers 5 variables: fuelburn and flight time incorporated with the environmental objectives CO_2, NO_x, and contrails. The framework allows for analysis and visualization of highly dimensional system outputs, *Y*, as shown in Figure 6. Apart from a baseline framework, there exists a version of the framework that is adapted for systems with multiple stakeholders and with internal optimization. This study utilized this version of the framework with optimization.

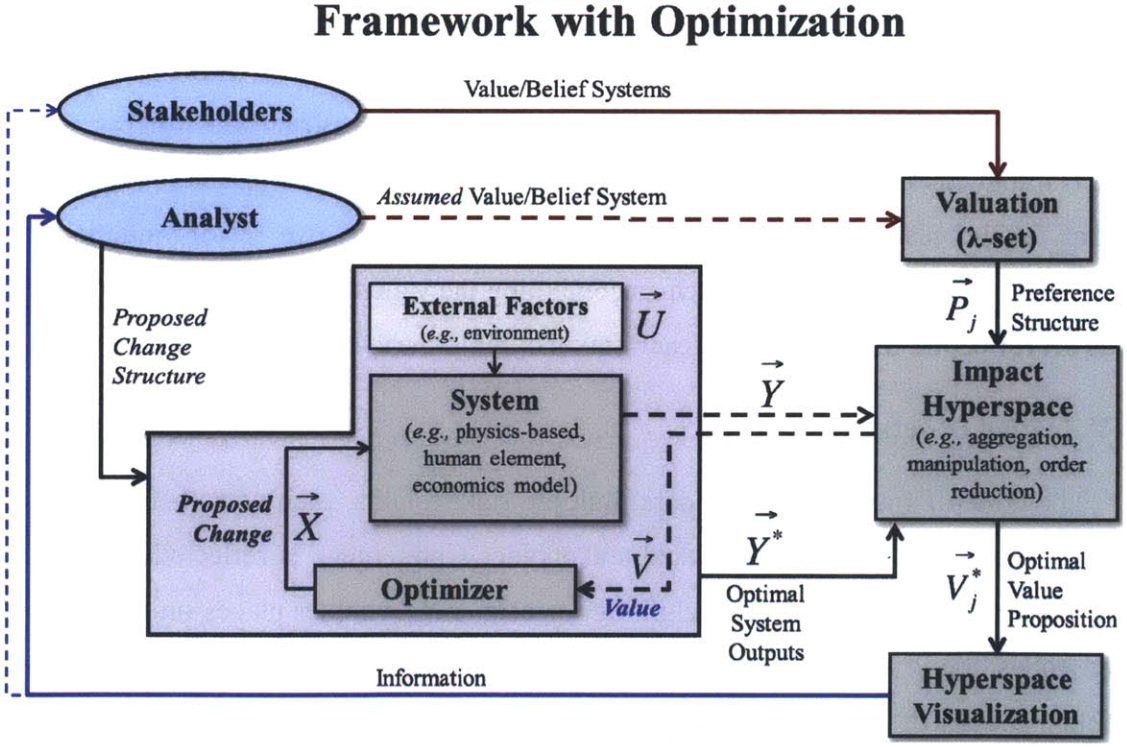

Figure 6 Tradeoff framework with optimization for multiple stakeholders.

In this approach the user of the tradeoff framework is an **analyst**, such as a researcher interested in the tradeoff problem. The analyst makes *proposed changes* to a **system model**, which describes and represents the system of interest. This model is further contextualized to the tradeoff problem with **external factors**, which creates a full simulation environment to generate

the *system outputs,* $\vec{Y}$. In the cruise operations optimization problem, the system outputs are fuelburn, flight time, CO_2, NO_x, and contrails. The analyst also has an *assumed value and belief system* for the tradeoff objectives that can be formalized into a set of **valuations**, called a *preference structure*. The preference structure is the value of cost the analyst places on the tradeoff variables. The system output and the preference structure are aggregated to form the tradeoff space termed **impact hyperspace**. In this space, the system outputs are presented reflective of the assumed value the analyst imposed on each tradeoff objective. With further exploratory data analysis such as dimension reduction, an otherwise hyperdimensional tradeoff space may be visualized. Such **hyperspace visualization** allows the analyst to obtain the necessary information for decisions on proposed changes and assumed value and belief system, thus completing the closed-loop framework.

The tradeoff framework used in this research also has an **optimizer** for finding the most valuable proposed change given a set of valuation. Under this framework, the analyst is no longer responsible for determining the proposed changes. Instead, the analyst inputs the necessary initial condition the optimization algorithm needs to find the optimal proposed changes. Note that for the case of multiple stakeholders each with their own set of valuations, a wide variety of approaches can be taken such as combining the valuation sets together into a weighted average set reflecting the influence of each stakeholder to the system of interest.

2.9.1 Valuation (λ-set)

The tradeoff framework considers multiple stakeholders, each with their own respective value and belief system. Each individual stakeholder's preference is reflected in the valuation component of the framework. The weighting, or cost, a stakeholder places on every variable is referred to as the λ of the variable, which makes the group of valuation for a particular stakeholder the set of λ, or **λ-set**. The analyst may choose to input a number of assumed value structures reflective of the different stakeholders with interest in the system for an exploratory purpose.

The purpose of the valuation is to reflect the stakeholder's preference structure. The approach taken in this research has the objective function, V, as a linear combination of the individual stakeholder's variable cost, λ_i, and the system output, Y_i.

$$V = \sum_{\forall i} \lambda_i \cdot Y_i$$

Therefore, depending on the weighting of preference structure on each tradeoff variable, the resulting objective function cost will reflect the relative importance the stakeholder places on each variable. The valuation becomes important in this research since there are two fundamentally different objective questions it is trying to answer. To do so, two valuations are used in this research to reflect two different stakeholders. For the contrail tax impact study, the stakeholders are the cost-driven players in aviation such as airlines and other aircraft operators. For them, the most important objective is to maintain cost-optimal operations. Therefore, as suggested by the cost index concept introduced in Chapter 1, the most important tradeoff variables currently are fuel burn and flight time. Fuel burn incurs fuel cost that has risen substantially in recent years. Flight time relates to block operating time that includes crew, maintenance, and aircraft cost. The objective of this research is to incorporate environmental costs to the traditional operation tradeoffs, with the research focus on contrails. This can be accomplished by adding the emissions and contrail cost to the valuation.

On the other hand, for environmental interest groups such as the Intergovernmental Panel on Climate Change (IPCC) whose authority on policymaking is based on climate impact assessments, the valuation changes to reflect the importance of the climate impact of emissions and contrail production. In order to measure the climate impact of operations, dollar cost is no longer sufficient and instead AGTP is used. The valuation in this study maps the system model outputs into the impact hyperspace as AGTP measurements that quantify climate impact as a global temperature change.

Chapter 3 - Methodology

The cruise phase flight level optimization tool developed in this research uses the tradeoff framework with optimization to incorporate contrails and emissions as additional variables to the traditional route optimization method that trades between fuel consumption and flight time. This section details the various components of the tool such as the system model and the optimizer. There are two versions of the system model used to conduct analysis for the two main studies: contrail tax impact study and climate impact study. While the two versions are similar in most aspects, there are some differences in the data sources and the calculating of the optimal profile that will be detailed in this section. Before the two studies are presented, a preliminary study using principle component analysis (PCA) is presented to illustrate how the fuelburn, flight time, and emissions correlate with contrail production.

3.1 Tradeoff Framework with Optimization

To implement the tradeoff framework to the cruise phase optimization problem, the first step is to construct a robust modeling environment that accurately reflects the cruise phase of flight. The modeling should be able to fly a mission and produce the desired outputs, namely fuel

consumption, time of flight, CO_2 and NO_x emissions, and distance through contrail regions, of typical missions with high fidelity (Figure 7).

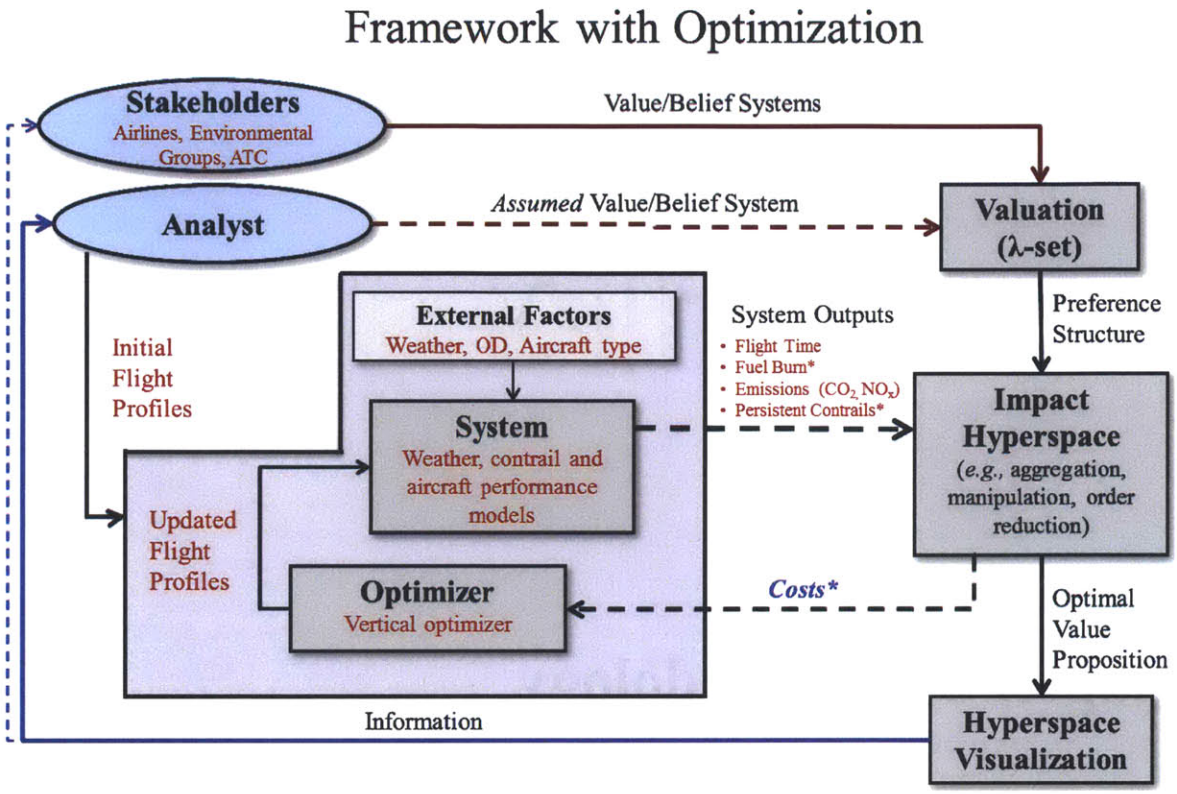

Figure 7 Tradeoff framework with optimization contextualized to the cost-based version of the cruise phase altitude optimization problem. *denotes where the metric changes from dollar cost to AGTP for the AGTP-based version.

With five tradeoff variables to consider, this optimization problem is computational complex, which makes parsing for the full output solution space computationally infeasible. Instead, only the optimal solution space is parsed using the tradeoff framework with optimization. By approaching the cruise optimization as a graph search problem where the nodes are transition points to remain level, climb, or descent and the arcs are the incremental path along the flight, the vertical optimizer developed for this study uses an iterative shortest path heuristic that finds the cost-minimal flight profile. In order to achieve the different objectives set out in this research, the cruise phase altitude optimization problem was approached using two sets of valuations (λ-set) reflecting two different stakeholder perspectives. The λ-sets are the distinguishing factor between the cost-based and AGTP-based versions.

3.2 Data Sources

The system model integrates a variety of data sources for weather, contrail, and aircraft modeling. The goal is to create a realistic physics-based modeling environment that can generate accurate outputs for cost and climate impact analysis.

3.2.1 Weather Data

To fully model the cruise operations, it is important to account for the ambient temperature, pressure altitude, and wind along the flight path in determining the groundspeed of the aircraft. Furthermore, ambient temperature and relative humidity are needed in modeling the contrail formation regions of the airspace. The necessary weather information is gathered from two forms of weather data provided by the National Oceanic and Atmospheric Administration (NOAA).

In the contrail tax study, the weather data used was the North American Regional Reanalysis-A (NARR-A). NARR-A is a re-analysis data product from the web-accessible National Operational Model Archive and Distribution System (NOMADS) data archive. The data are generated by assimilating observations and satellite data of the past atmospheric conditions of North American region. It is the most accurate source of historic data with information on temperatures, winds, pressure, and humidity, amongst other things. Re-analysis data such as NARR-A is most appropriate for the purpose of this study of modeling historic weather days.

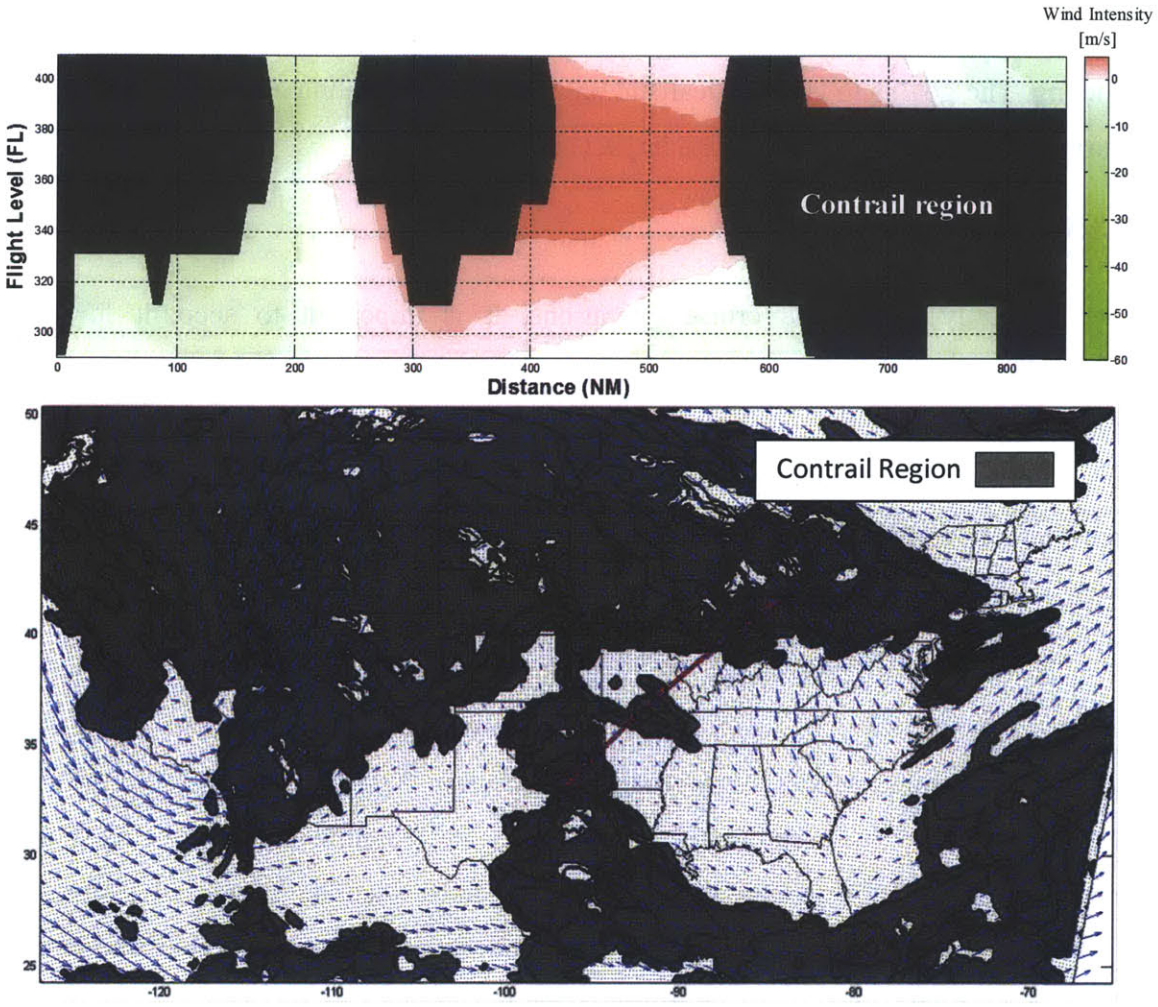

Figure 8 Representative weather using RUC data: Wind optimal DFW-DTW on a B733 for April 10, 2012 at 16UTC. The top plot is the vertical profile of the flight showing the wind intensity (green & red) and contrail forming regions (gray). The bottom plot shows the map view of the flight with the wind vectors shown as quivers and the contrail forming regions (gray) stacked from FL280 to FL440.

In the climate impact study, where the environmental impact of contrails was evaluated, the data came from NOAA's weather prediction model called Rapid Update Cycle (RUC) as shown in Figure 8. RUC data are mainly used when the weather forecasts are of interest, which is not the case for this study. RUC was used in an effort to conform to the data source of our collaborators at NASA Ames for the sake of comparison; they have developed a lateral optimizer for cruise operations complementary to our vertical optimizer. Since the forecasting feature was not used, only the RUC initial conditions were parsed for weather modeling. In regards to the

disparities between the two data sources, aside from negligible temporal and spatial resolution differences, the outputs are similar (Table 1).

Table 1 Notable differences between the data parsed from NARR-A and RUC 20km.

	NARR-A	**RUC 20km**
Spatial Resolution	32 km X 29 pressure levels	20 km X 37 pressure levels
Temporal Resolution	3 hour updates	1 hour updates
Years available	1979 - 2012	2002 - 2013

The file format of both weather data types is Gridded Binary (GRIB), a standard for meteorological data and has two generational versions, GRIB and GRIB2. The map grid of the weather data is of the North American region and is projected using lambert conformal conic, which is preferred in gridding middle latitude regions for its accurate portrayal of distance and spacing. Aeronautical charts typically use this type of projection; i.e. a straight line on a lambert conformal conic map is a great circle track. The interpolation of the weather data from the data grid along the flight track is a nearest neighbor approach as shown in Figure 9. For example, the weather data used to generate the wind in the top plot of Figure 8 is interpolated from the lateral track for FL290 to FL410 (8 of the 37 pressure level data layers) shown in the lower plot.

3.2.2 Contrail modeling:

The persistent contrail modeling for the operating cost portion of this study applied the RH_w and RH_i criterions, which is an adequately modeling approach when compared to satellite observations (Degrand & Carleton, 1977-1979). However, this simplification it does not capture contrail dispersion that occurs under realistic atmospheric conditions. Recent advancements in contrail modeling have been able to incorporate Lagrangian particle dispersion model and cloud microphysics model to capture this spreading effect. NASA Ames, the author's collaborators on a portion of the climate impact study, extended the simplified persistent contrail model to include this dispersion modeling and provided us with the contrail data for analysis in the climate impact study. The contrail regions generated for Figure 8 and Figure 9 used this contrail model.

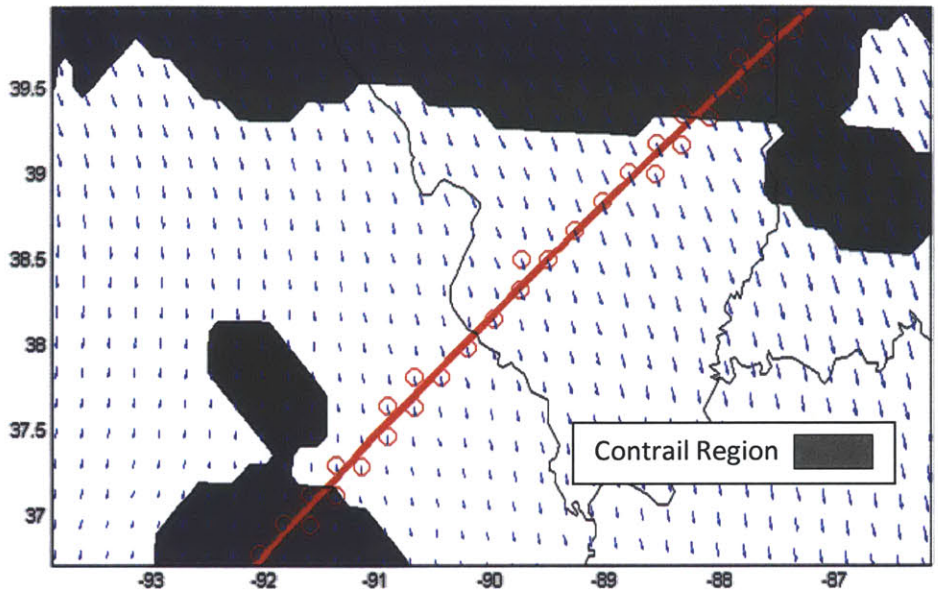

Figure 9 Airspace over Missouri and Illinois, mid-cruise for the DFW-DTW flight showing the map grid with the lateral track and contrail region for FL390. The wind vectors are shown in quivers. The circled points are the closest data points to the track from which the weather data is interpolated and used to generate the vertical weather profile depicted in the top of Figure 8.

3.2.3 Aircraft performance modeling:

Another aspect of the cruise operations that requires modeling is the aircraft performance characteristics. The fuel burn is very dependent on the aircraft type, as are the operating time and emissions. The tool used in this study is Project Interactive Analysis and Optimization (Piano-X) developed by Lissys. This professional aircraft analysis tool has a wealthy inventory of existing aircraft types along with high-fidelity aerodynamic and performance data for each aircraft.

Using Piano-X, aircraft performance data are exported as lookup matrices with dimensions of gross weight (ranging from operating empty weight to maximum takeoff weight), altitude (FL290 to FL410), and Mach number (minimum and maximum allowable per aircraft). The performance variables of interest to the analysis include the specific air range (SAR) and NO_x emissions index. SAR, the distance traveled per unit of fuel used, makes a direct relationship between the fuel consumption with the distance traveled. By using wind-corrected distance flown, the fuel consumption can be integrated. The SAR value extracted from Piano-X uses values assuming default cruise condition.

To find the NO_x emissions output, the emissions index is extracted from Piano-X. This index defines the grams of NO_x produced per kilogram of fuel used. Based on the flight condition, Piano-X uses the Boeing fuel flow method 2 (Boeing 2) to calculate the emissions index relative to a reference index value from the ICAO databank. Boeing 2 is an emissions estimation method that uses non-proprietary engine emissions characterization to approximate emissions to within 10 to 15% of estimates generated from proprietary modeling, which are superior due to higher quality of data. Note that CO_2 emission is directly proportional to fuel burn; 1 kg of jet fuel produces 3.16 kg of CO_2.

A total of 11 aircraft types were used in this research. Their lookup matrices were generated from Piano-X and used in the aircraft performance model integrated in the system model (Table 2).

Table 2 All aircraft types used ordered by MTOW. The preliminary and contrail tax studies used all of the aircraft, whereas the climate impact study used the aircraft types shaded in green.

	B737-300	B737-700	B737-800	MD83	A319	A320	B757-200	B767-200ER	B767-300ER	A330-200	B777-300ER
Seating Capacity	150	215	215	172	156	180	239	255	350	380	550
Length (m)	33.4	42	42	45	34	38	47	48.5	55	59	74
Wingspan (m)	28.9	36	36	32.8	34	34	38	47.6	48	60	65
Operating Empty Weight (lbs)	72100	74000	74000	79700	90000	107000	128000	181610	198000	264000	370000
MTOW (lbs)	138500	150000	150000	160000	166000	170000	255000	395000	412000	520000	775000
Cruise Mach	0.74	0.74	0.74	0.76	0.78	0.78	0.8	0.8	0.8	0.82	0.84
Max Range (NM)	2300	2400	2400	2500	3600	3200	3900	6385	6000	7250	8000
Operating Cost* ($/BLK hr)	1900	1700	2000	2000	1900	2000	2500	2800	3300	2900	4000

3.3 System model

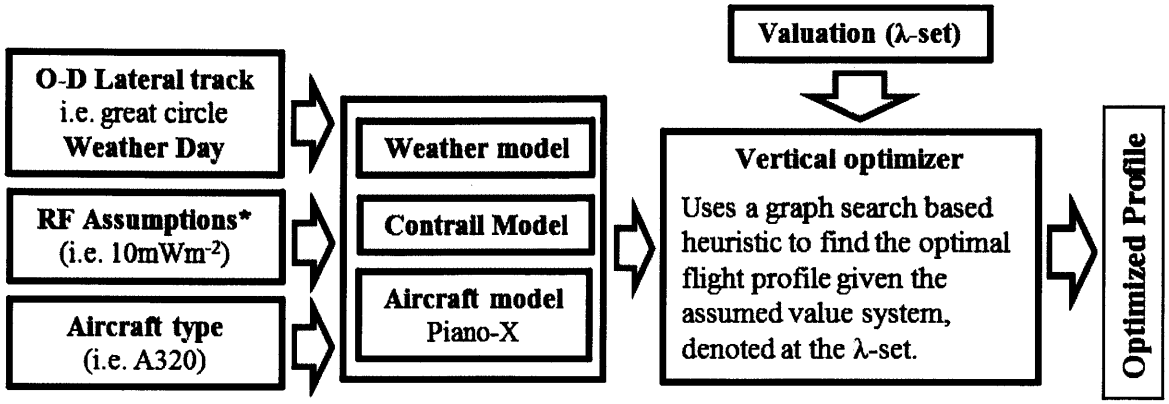

Figure 10 The system model of the tradeoff framework with optimization adapted to the cruise problem encompasses the external factors, the various models, and the optimizer. * The contrail RF assumption only applies to the climate impact version of the system model.

Weather, contrail, and aircraft modeling create the simulation environment for the cruise phase of flight, with robustness to handle a variety of weather conditions, O-D pairs, and aircraft types. The system model, shown in Figure 10, integrates this environment with a shortest path heuristic in a closed loop feedback to optimize these missions. The external factors specify the lateral track and weather day of interest, the system model extracts the along-track wind vector, temperature, and relative humidity for every pressure altitude that is available for flight level change from the NARR-A/RUC database described in the previous section. Based on the type of aircraft specified to fly the particular mission, the aircraft performance characteristics throughout the cruise mission can be obtained from the lookup table generated from Piano-X. The cruise operation modeled in this study is discretized by the number of flight level changes (2000 ft. increments) and along-track transitions points dictated by the distance traversed by the aircraft climbing or descending to an adjacent flight level. This suggests that the flight level optimization problem could be approached as a shortest path problem with a graph network of transition points where the aircraft has the choice of ascending, descending, or maintaining level cruise. The heuristic used is a k-shortest path (KSP) algorithm based on Dijkstra's graph search method. Due to the weight-dependent nature of aircraft performance, interim flight profiles found by the algorithm were automatically flown iteratively until the weight profile converges to a final optimal flight profile. The optimal profile is found by evaluating the cost by applying a cost

structure to the system outputs of fuel burn, operating time, CO_2, NO_x, and contrail produced until a minimum cost is found.

For the contrail tax study, the cost structure, or λ-set, uses the most current fuel (λ_{fb}), block operating (λ_{oc}), and emissions and contrail social costs (λ_{co2}, λ_{nox}, λ_{cont}) in dollar per unit output. In the climate impact study, the λ-set consists of only λ_{fb} and λ_{cont} in AGTP unit of kelvin of temperature change per unit output. The outputs are evaluated in the impact hyperspace where the tradeoff solution space is generated by the system model.

3.3.1 Defining the Cruise Profile

The cruise profile for flight level optimization can be constructed into a directed graph from origin (start node) to destination (end node). For a directed graph *G(N,A)*, the nodes, *N*, are all the possible altitude change points along the flight profile and the arcs, *A*, joining the nodes are incremental paths along the flight with costs associated with them. The arc costs are based on the linear combination of the individual outputs with their perspective valuation, normalized to the distance of the incremental path.

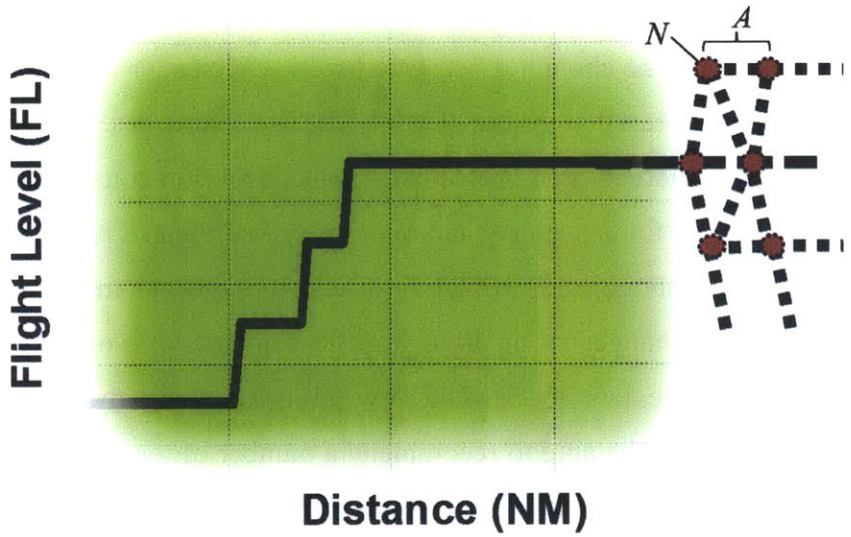

Figure 11 Visualization of the graph network of a cruise profile. Each node, *N*, is the aircraft's transition point to climb, descent, or remain level. The arc is associated with the incremental path distance it takes for the aircraft to climb to the next flight level (+200ft).

$$\text{Arc Cost} = \lambda_{fb} \cdot Y_{fb}[gal] + \lambda_{oc} \cdot Y_{oc}[sec] + \lambda_{CO2} \cdot Y_{CO2}[kg] + \lambda_{NOx} \cdot Y_{NOx}[kg] + \lambda_{cont} \cdot Y_{cont}[NM]$$

The distance of the incremental paths is variable to the assumed average climb rate of the aircraft. Based on the climb rate, the incremental path distance is the distance the aircraft traverses to climb to the next flight level (+2000 ft.). For the case of an A320, the path distance is roughly 7.5 nautical miles. Therefore, here we made the simplifying assumption that the descent distance is the same as the climb distance. In real life, typically descent rates are faster than climb rates, as the operator often want to maximize the fuel efficiency of the higher altitude before dropping to a lower flight level. Furthermore, the climb and descent aircraft performance characteristics are assumed to be a coefficient factor of that of level cruise. Based on a previous study, these coefficient factors were shown to match Piano-X calculations with good accuracy.

Table 3 Cruise phase climb and descent coefficients (unitless) used to estimate non-level flight performance characteristics

	Climb	**Descent**
Fuel burn & CO_2	**1.215**	**.79**
Flight time	**1.003**	**.998**
NO_x	**1.43**	**.66**

3.3.2 Vertical Optimizer Heuristic

The first criterion for the choice of heuristic used is efficiency. The algorithm that comes to mind is Dijkstra's graph search algorithm, mainly for its relative ease in implementation and its wide use in analogous shortest path problems. Another criterion considered in the choice of heuristic is the capability of finding more than one optimal solution. The need for multiple top solutions roots from the highly constrained nature of cruise operations in real life; i.e. limitation on the number of altitude changes from the air traffic controls or avoidance of heavy traffic altitudes over an airspace region, to name a few. Without explicitly considering for each constraint, the heuristic should be able to recommend a number of top solutions for the operator to choose from as an advisory tool, allowing the operator to decide based on the constraints of each scenario. Most single shortest path algorithms such as A* grow exponentially in computation time with each additional solution, making them rather cumbersome to run if more than one solution is desired. Therefore to satisfy the second criterion, the system model uses the k-shortest path (KSP) algorithm (Yen, 1971). This algorithm is specifically designed for finding k number of solutions without sacrificing computation time with additional solutions. In fact, the computation time grows linearly with increase in k (Figure 12).

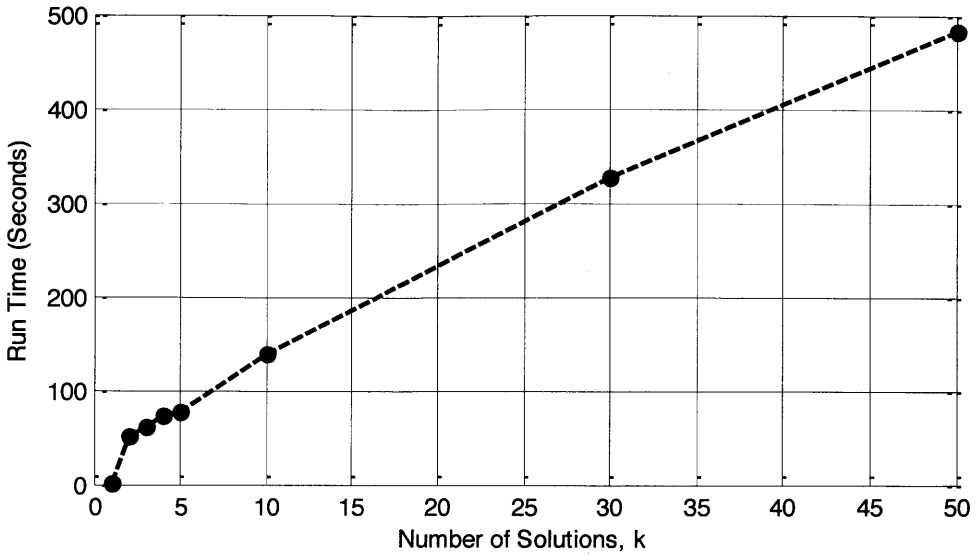

Figure 12 The runtime of each additional solution using KSP grows linearly as opposed to the exponential growth of single solution graph search methods.

3.3.3 Weight Convergence

Since the aircraft performance characteristics are dependent on the weight of the aircraft, a feedback loop is needed to ensure convergence of the gross weight profile. This is due to the path-dependency of the gross weight; depending on the flight profile taken to get to a point along the flight, the gross weight of the aircraft and subsequently its performance characteristics changes. The goal is to iteratively fly the optimal profile found by the heuristic for convergence to a realistic weight profile. The initial gross weight profile inputted into the optimizer is that of a worst-case scenario 1800NM mission at maximum allowable Mach speed and FL290 flown in Piano-X. Since 1800NM is longer than most missions flown for this study, the top of climb (TOC) weight for the initial gross weight profile is in general an over-estimation for other missions used in this study, making it a bad reference weight for convergence. Instead, the top of descent (TOD) weight at the end of the worst-case scenario flown in Piano-X is use. This weight is not as dependent on the trip length and provides a better reference weight for convergence. The approach of this iterative step is as follows:

Step 1: Find the interim optimal cruise profile using an initial aircraft gross TOC weight from Piano-X, which simulated a worst-case 1800NM mission profile at maximum allowable Mach speed and FL290.

Step 2: Then fly the profile to obtain the total fuel burn weight from the first profile.

Step 3: Add this total weight of fuel burn to the TOD weight from Piano-X, creating a new top of cruise weight more suitable for the mission. Note that this total fuel burn weight is found using the over-estimated TOC weight, therefore the new 'lighter' weight profile will, at most, burn the same amount of fuel. Find the new interim optimal cruise profile using the new TOC weight.

Step 4: Iterate steps 2 and 3 while keeping track of the change in the weight profiles until the weight profile of the optimal solution converges.

3.4 Study-specific System Models

There are two versions of the system model used in this research, specific to the two main studies: Contrail tax impact study and climate impact study. The framework remains the same for both versions. The distinctions lie in the valuation (λ-set) to reflect the different perspectives of the two studies, plus the weather and contrail model used.

3.4.1 Cost-based Optimization

In the cost-based version, the system model is designed for the contrail tax impact study to optimize based on an operating cost based objective function (Figure 13). That is, every tradeoff variable is valued in dollar cost. The intent is to explore the various cost-based tradeoffs associated with contrail avoidance; namely, the total operating cost and additional fuel cost tradeoffs.

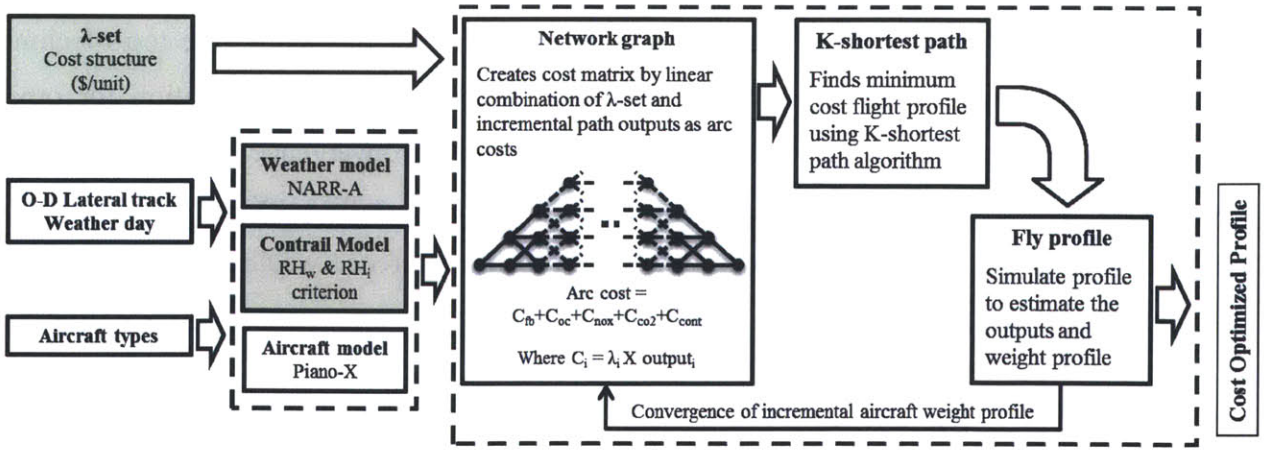

Figure 13 The cost-based system model used in the contrail tax studies. The distinctions from the climate impact portion lie in the λ-set, the resulting network graph, and weather and contrail modeling (shaded).

The λ-set used in the cost-based system model comes from the latest estimates of jet fuel price from International Air Transportation Association (IATA), block operating cost for specific aircraft type, social cost of CO_2 from the U.S. Environmental Protection Agency and NO_x from the Department of Energy (Table 4). There is no current estimate on the social cost of contrails.

Table 4 The latest estimates of variable costs make up the λ-set used in determining the operating cost of contrail avoidance.

λ_{fb}	λ_{oc}	λ_{CO2}	λ_{NOx}	$\lambda_{contrail}$
Jet Fuel Cost	Block Operating Cost	Social Cost of Emissions		
3.00 $/gal	i.e. A320: 2000 $/Bhr	0.023 $/kg	4.05 $/kg	? $/NM
IATA	*2012 Aviation Week AOC & S*	*SCC from US EPA*	*DoE estimate*	

The weather model used in the cost-base system model is the NARR-A reanalysis data from NOAA. The contrail model is based on the relative humidity criterions discussed in detail in Chapter 1. The arc cost calculated in the network graph is a linear combination of the λ-set and the outputs of all five tradeoff variables. In the contrail tax study, the cost-based system model is used to analyze the impact of different cost of contrails on the optimal flight profile.

3.4.2 AGTP-based optimization

For the climate impact study, instead of the dollar cost metric used in the cost-based version, the AGTP-based system model is used to generate optimal profiles that are evaluated in terms of AGTP, a climate impact metric that measures the instantaneous change in the global temperature due to a radiative forcing (RF). The AGTP-based system model is used to tradeoff between the benefit of contrail avoidance and the negative impact of CO_2 emissions measured at different climate impact time horizons under various contrail RF estimates.

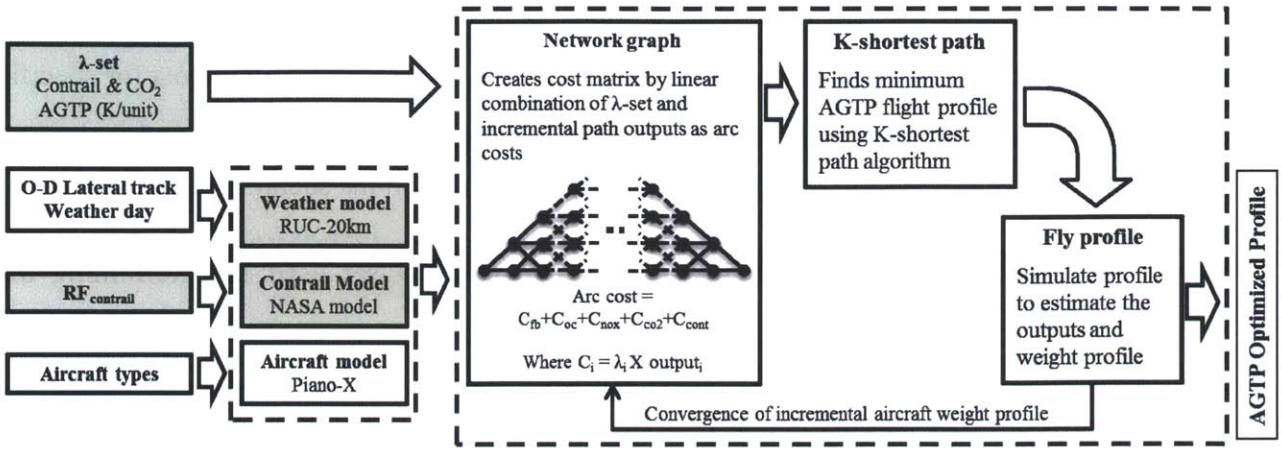

Figure 14 The AGTP-based system model where the λ-set reflects the change in surface temperature in kelvin per kilogram of fuel burnt or nautical mile contrail produced. The weather data used in this model is the RUC-20km. The distinctions from the cost-based system model are shaded.

The λ-set used in the AGTP-based system model includes only the AGTP valuation for contrails and fuelburn. The other three variables flight time, CO_2 and NO_x are set to 0 for this system model as they either have no direct climate impact or they are negligible compared to contrails and fuelburn for the purposes of this research. The AGTP valuation for contrails is in the unit of kelvin per nautical mile of contrail produced. The values are generated by NASA Ames using their more advanced contrail model.

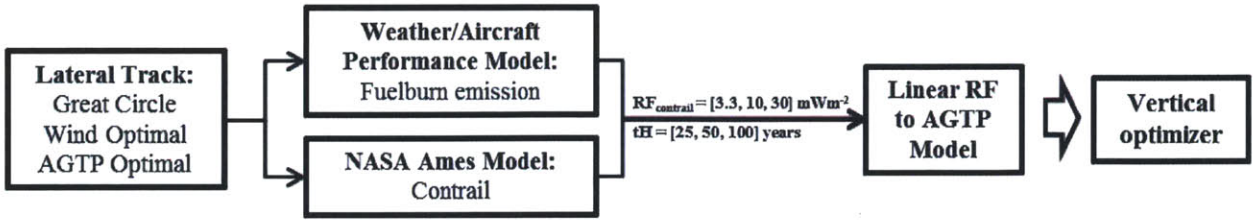

Figure 15 The choice of contrail RF determines the AGTP due to contrail. The choice of time horizon to optimize affects the AGTP due to contrail and fuelburn.

Recall from Chapter 2 that 3 values of contrail RF are used in this research to determine the sensitivity of the optimal profiles to different contrail RF values. Furthermore, also recall that since the climate impact of contrails and CO_2 are different dependent on at what time horizon the measurement is made, 3 different time horizons are considered in this research. Therefore, there are a total of 9 sets of AGTP values for contrails depending on the contrail RF and time horizon

specified (Figure 15). The AGTP valuation for fuelburn is in the unit of kelvin per kilogram of fuelburn and also varies based on the time horizon (Table 5).

Table 5 The AGTP valuation of fuelburn by different time horizon of climate impact

Time Horizon [years]	$AGTP_{fuelburn}$ [K/kg]
25	2.1132E-15
50	1.8207E-15
100	1.5983E-15

3.4.3 Illustration of the system model solutions

This section illustrates the outputs of the system model by implementing the cost-based and AGTP-based optimizer on a representative mission. The goal is to verify that the system model works correctly.

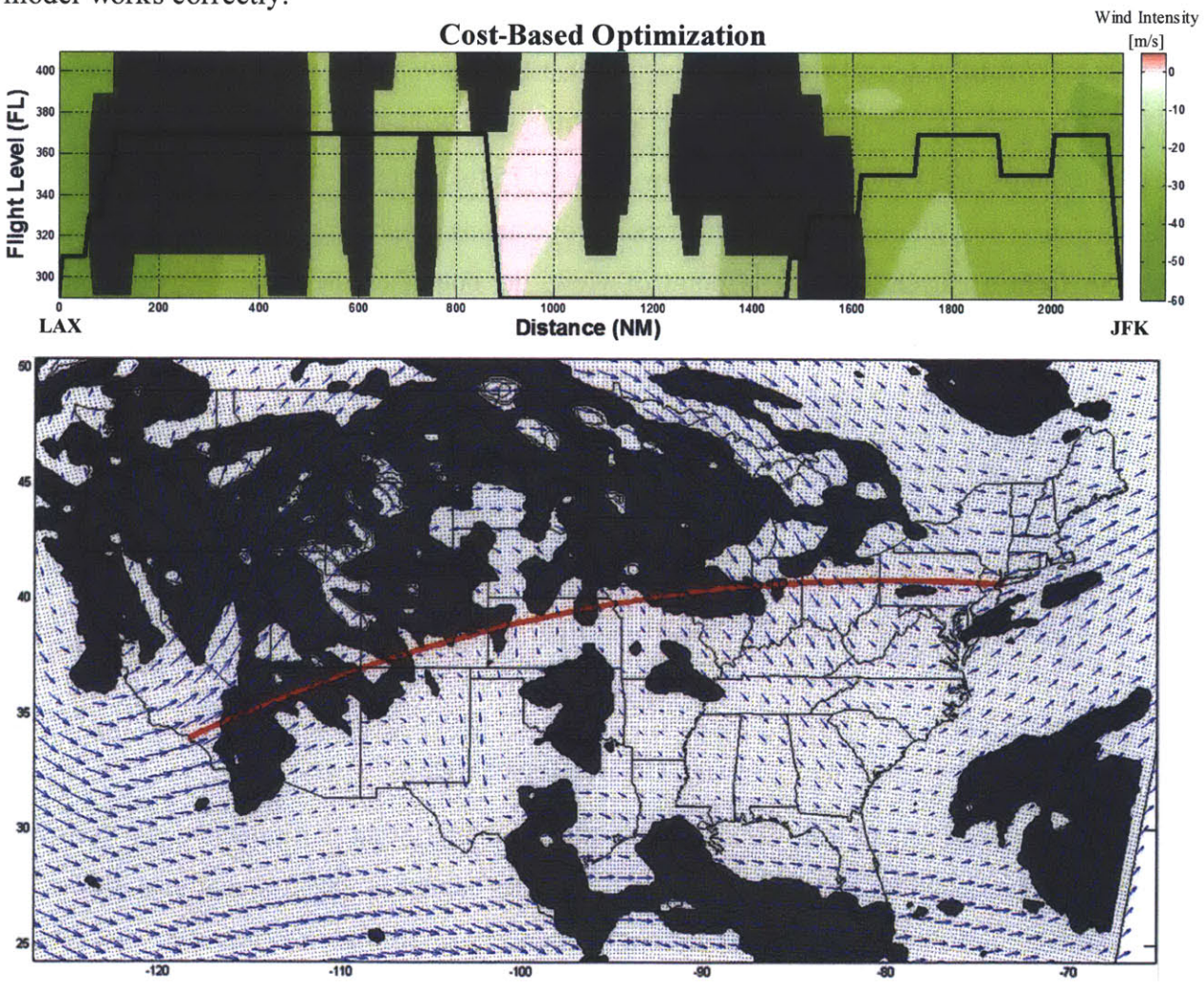

Figure 16 Representative flight profile from LAX to JFK on the A320 along the great circle track calculated using the cost-based optimizer. The flight levels range from FL290 to FL410. This is the fuel-optimal profile found by setting all costs to zero except for fuelburn. Contrail region shaded in gray.

The example used is a LAX to JFK flight on the A320 at April, 12, 2010. The goal of this example is to verify that the system model is working correctly compared to traditional profiles, therefore contrail avoidance should not be considered for this case to avoid complexity. As shown in Figure 16, the profile flown is the most fuel efficient profile, which is found by setting every variable cost in the λ-set except fuelburn to zero. Therefore, by mapping all of the possible flight profiles to this λ-set, this profile is the cost minimal. Note that it flies wind optimal by avoiding headwind and flying in strong tailwind regions. It turns out that this profile is identical to the total operating cost optimal profile found if all variable costs are set at the current standards (Table 4), with the contrail cost set to 0$/NM. This suggests that the current cruise phase optimization problem is mostly driven by the jet fuel cost. In comparison to current operations, this complies quite well with typical profiles flown by airlines. Referring back to the cost index (CI) discussed Chapter 1, it turns out that Boeing 757 typically flies a CI between 15 and 50, where the full range of the aircraft spans 0 to 999 (Roberson, 2007). Since a CI of zero denotes the most fuel efficient profile, a low range of 15 to 50 means fuelburn cost is prioritized over operating cost and that the current standard operations emphasizes fuel efficiency to flight time. So from a current operations point of view, the output of the system model complies reasonably well.

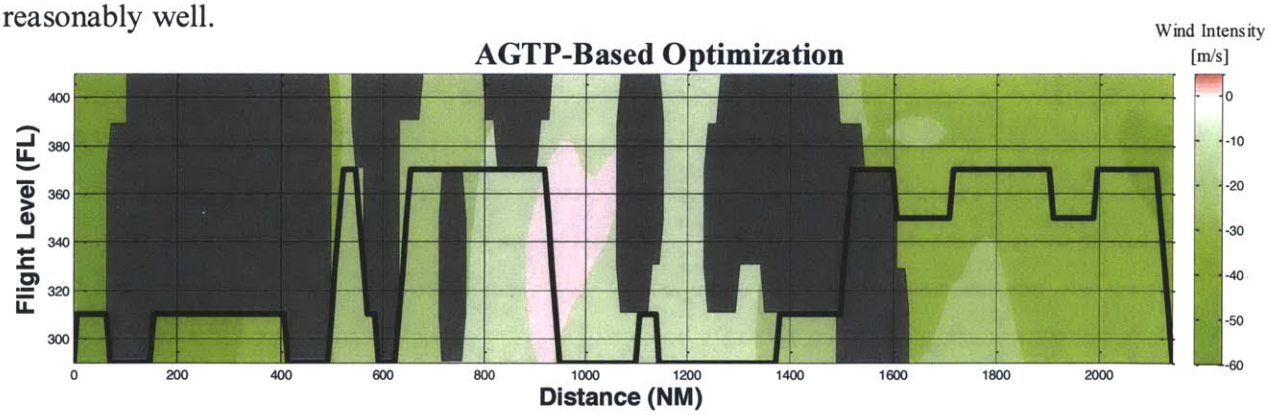

Figure 17 The same representative flight, here using the AGTP-based optimizer. The contrail RF = 30mWm^{-2} and time horizon of 25 years. Contrail region shaded in gray.

As can be observed from Figure 17, the AGTP optimal flight profile is one that considers contrail avoidance. Note that a downside to the system model is that it sometimes allows for irregular and unrealistic climb and descent sequences. In the sample mission, the aircraft oscillated between FL290 and FL370 twice around 500NM to 600NM along the flight. In the implementation of the optimizer, a constraint is applied to not allow 'spikes', climb followed by descent with no level cruise and vice versa, to exist in the flight profile to avoid unrealistic

optimal profiles. This constraint is applied by way of a post-output filter. This filter identifies a series of 3 or more altitude changes with interchange signs (+,-,+ or -,+,-) and recalls the system model to generate additional solutions until a feasible solution is obtained. This step is made computationally simple with the KSP algorithm. While detecting infeasible altitude changes is a simple constraint to implement, more complex rules such as limiting the number of altitude changes within a certain distance of the trip are less obvious to implement due to the inherent ambiguity in the standard rule. In real-life operations they may differ depending on the region of the airspace regulations and air traffic controller.

3.5 Correlation of Variables

Before the two main studies, it is important to rigorously establish the relationship between the 5 tradeoff variables in this research. The findings of this study will establish the main variables the subsequent studies should use to conduct tradeoff analysis with contrail production. To explore the correlations between the tradeoff variables, principle component analysis (PCA) was conducted. PCA is a dimensional analysis tool that is typically used for dimensional reduction of highly dimensional data. To do this, the fundamental mechanism of PCA is to find linearly uncorrelated basis, the principle components, onto which the data can be most efficiently represented. For example, if a 3-dimensional data include 2 variables that are highly correlated, PCA is able to recognize that this data set can be represented with only two dimensions without losing too much information in the 3-dimensional space. For our purposes, PCA is used to reduce the 5-dimensional full solution space we obtained from a simplified version of the system model into a visualizable 3-dimensional space while preserving the main correlations between the 5 variables (Figure 18). The solution space is populated by solving for every variation of the λ-set ranging from 0 to a projected upper bound of each variable. The solution space consists of outputs in appropriate units for each tradeoff variable. The outputs are subsequently normalized from 0 to 1 to avoid skewing the observed variance due to the different units of measurements. The source of the projected upper bound is given as marked by * below:

$\lambda_{fuelburn}$	$0 \rightarrow 3.18$ [$/gal]	* EIA AEO 2025 projection of $3.18 per gal
$\lambda_{flight\ time}$	$0 \rightarrow 3400$ [$/BHr]	* 2012 AOC&S using B747-400 $3400 per BHr
λ_{CO2}	$0 \rightarrow 0.5$ [$/kg]	* Gov't working group project $0.5 per kg by 2050
λ_{NOx}	$0 \rightarrow 5$ [$/kg]	* DoE estimate upper bound at $4500 per metric ton
$\lambda_{contrail}$	$0 \rightarrow 2$ [$/NM]	* Preliminary estimate from contrail tax impact study

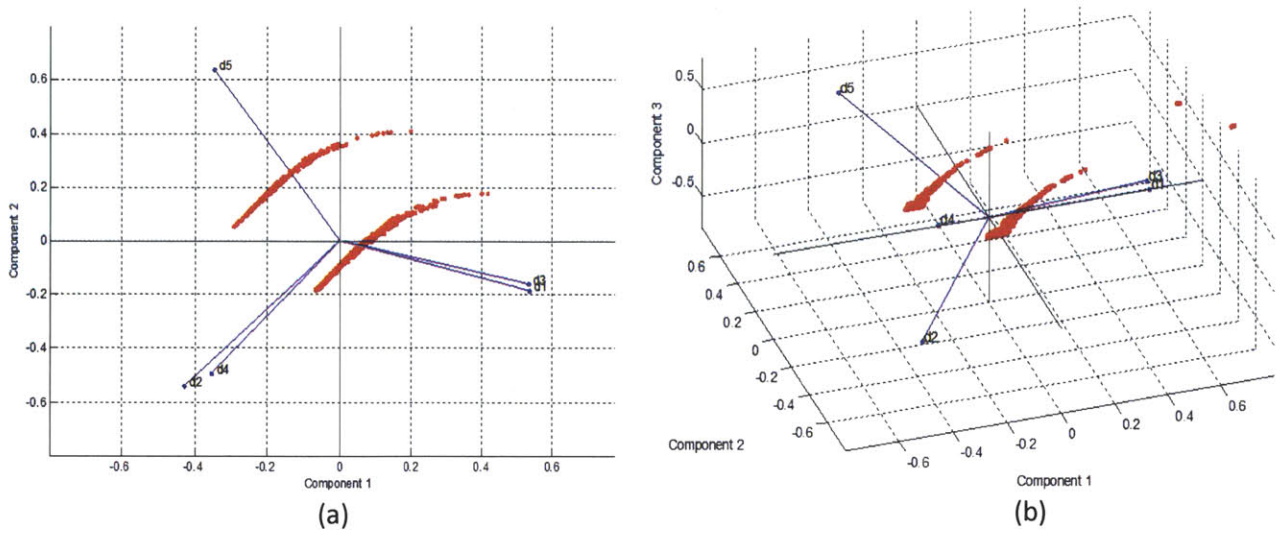

Figure 18 3-D visualization of the 5 tradeoff variable components using PCA for the day of 2/1/2009 and flying a A320. (a) A 2-D view of the optimal solution space projected on the principle components 1 and 2. (b) The optimal solution space projected in 3-D. Fuel burn (d1) and CO_2 (d3) are highly correlated. Flight time (d2) and NO_x (d4) are also reasonably correlated. Contrail production (d5) is less correlated to the other four variables.

By looking at Figure 18, it is clear that fuel burn (d1) and CO_2 emission (d3) are highly correlated, as expected. Additionally, flight time (d2) and NO_x emission (d4) are correlated, which supports results from other studies that suggest ozone formation (aircraft emitted NO converts to NO_2) drops with altitude (Kohler, 2008). The first principle component, which is the basis onto which the data has the most variance, is closely aligned with fuel burn and CO_2 emission. This suggests that fuelburn, and thus CO_2 emission, varies the greatest and carries the most information about the optimal solution space. Furthermore, since the component of fuelburn points almost opposite from that of contrails in the 2-D and 3-D space, fuelburn and contrail production are direct tradeoff variables. By the same logic, contrail production is nearly orthogonal to flight time, which suggests that these two variables have less correlation with one another.

The two cluster of solution is an artifact of the weather day used and the discrete nature of the solution space. The two clusters differ by the distance of contrail production because they lay along d5, the dimension of contrails. Referring to the weather condition on 2/1/2009 in Figure 20, one cluster of solution chose to climb immediately into the contrail region at the beginning of the flight and thus incurring a greater distance through contrail. The other cluster chose to avoid contrails by cruising at FL290 until contrail became unavoidable (See Appendix A). The correlations between the variable components are tested for 12 days, first day of every

month for the year 2009 (Figure 20), and the results are not drastically affected by these artifacts of the weather condition. The angles between the tradeoff variable components remain consistent independent of the weather day and aircraft type. To better show the data depicted in Figure 19, the results are tabulated in Table 6

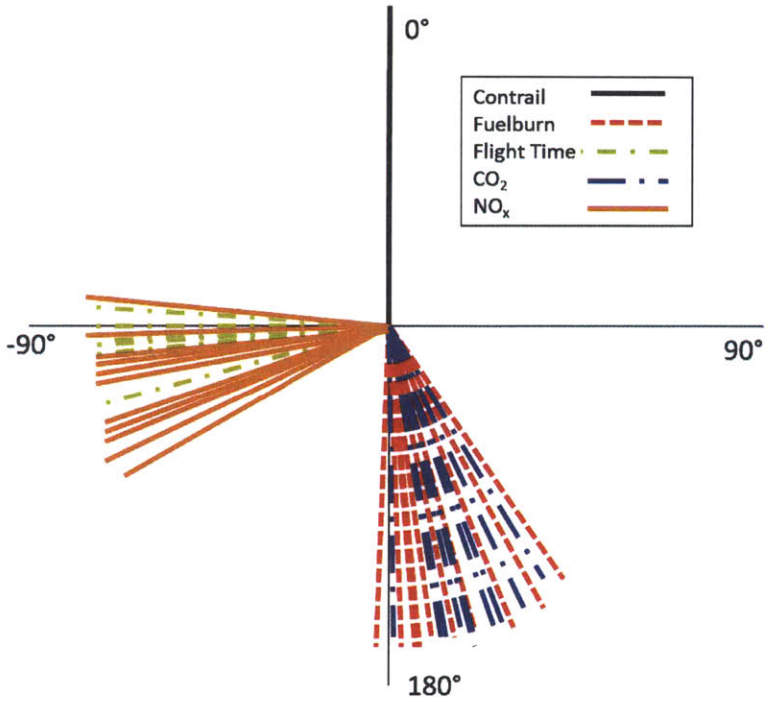

Figure 19 Using contrail as the reference angle of 0°, the angles of the other 4 variables are shown for all 12 weather days. The correlation between the variables is fairly consistent.

Table 6 Using the variable contrail as the reference angle of 0°, the other 4 variable components are projected in the2-D space of 1st and 2nd principle components for 12 days of 2009, similar to Figure 19.a. The range of angles for the different weather days is fairly consistent.

	Fuelburn	**Flight Time**	**CO_2**	**NO_x**
Minimum angle	147°	-86°	154°	-83°
Maximum angle	181°	-103°	179°	-120°
Range of angles	34°	17°	15°	27°
Mean angle	172°	-97°	167°	-103°

The main takeaways from the preliminary study are the following:

- Fuelburn is highly correlated with CO_2 emission and flight time is highly correlated with NO_x. Therefore an observation from one variable may likely be indicative of the behavior of the other.

- Fuelburn and CO_2 are highly correlated with contrails based on the nearly 180° angle between the variables. Therefore they should serve as strong tradeoff variables relative to contrails. This can be explained by the notion that the reduction of contrail production requires additional fuelburn to maneuver around contrail forming regions of the airspace.
- On the other hand flight time and NO_x are weakly correlated to contrails. Notionally, higher altitudes are denser with contrail forming regions due to the lower ambient temperature and correlates to longer flight time since the groundspeed per given Mach number is less at lower temperatures.

Chapter 4 – Contrail Tax Impact Study

The purpose of this study is to investigate the impact of contrail tax on current operations. With the implementation of contrail tax, contrail production becomes an additional variable of cost for jet aircraft operators to consider. Using the cost-based system model, this contrail production cost is incorporated to the traditional cost structure, alongside social costs of CO_2 and NO_x emissions. The goal is to explore the impact such a contrail tax has on the choice of the cost-optimal flight profile flown. Before beginning analysis on the impact of contrail tax on cruise phase optimization with contrail avoidance, first this study looks to establish a notion of the sensitivity of optimal profiles to various weather conditions and aircraft types. This sensitivity analysis will distinguish generalizable trends of contrail avoidance that are not artifacts of the weather and aircraft used. On the grounds of the preliminary study and these sensitivity analyses, this study attempts to derive a range of contrail tax price that should be implemented if taxation is used as a contrail mitigation policy.

4.1 Weather Sensitivity

In an effort to find out how contrail avoidance strategies vary with the weather condition of the day, a weather sensitivity analysis is conducted. Using the NARR-A database, 12 days of weather data from the first day of each month of 2009 were compiled for the along-track cruise

phase of an actual flown flight from LAX to JFK, altitude spanning from FL290 to FL370. The persistent contrail regions are found by the relative humidity criterions described in Section 2.1. The wind vector is defined as the along-track horizontal wind component. Therefore there is headwind, tailwind, or no wind relative to the aircraft. This simplifies the calculation of the wind-adjusted properties of the incremental flight path. For computational efficiency the wind vector is not readjusted for climb and descent. These 12 weather days make a representative mix of heavy and light contrail days; November has no contrail producing regions whereas January and February are nearly completely covered in contrail regions (Figure 20).

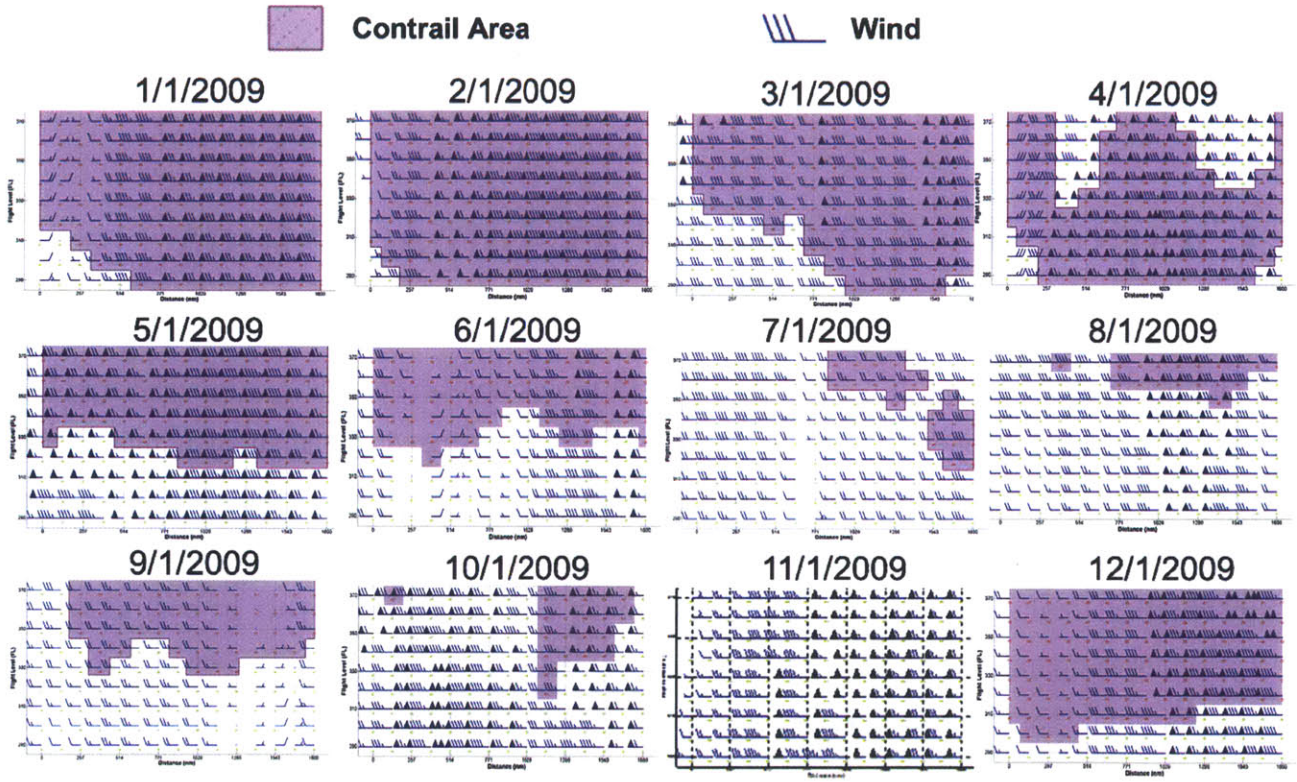

Figure 20 Weather days for LAX-JFK for the first day of every month of 2009. The contrail producing regions are shown in magenta and the wind intensity and direction shown in feathers.

A few observations are worth noting at this point. First, it appears contrail formation regions reside mainly at higher altitudes than lower ones. May through October weather days all have contrail-free flight levels around FL290 and are relatively dense with contrail-forming altitudes around FL370. Therefore the contrail minimal flight profile would likely fly at a lower altitude. This observation suggests that, in general, the contrail avoiding profile contradicts the

fuel optimal profile, which prefers flying at higher altitudes. Furthermore, presumably contrail avoiding profile may also reduce the flight time by flying at a lower altitude.

The weather sensitivity of contrail avoidance was approached by setting the λ-set to the current cost structure tabulated in Table 4 while varying λ_{cont}. The algorithm will tradeoff the cost of the distance of contrail traversed by the aircraft with the fuel cost, operating cost (here denoting by block flight time and without fuel cost), and emissions social costs. Intuitively, as the cost per unit distance of contrail produced, λ_{cont}, increases the algorithm will select optimal profiles that fly through less contrail forming regions (Figure 21).

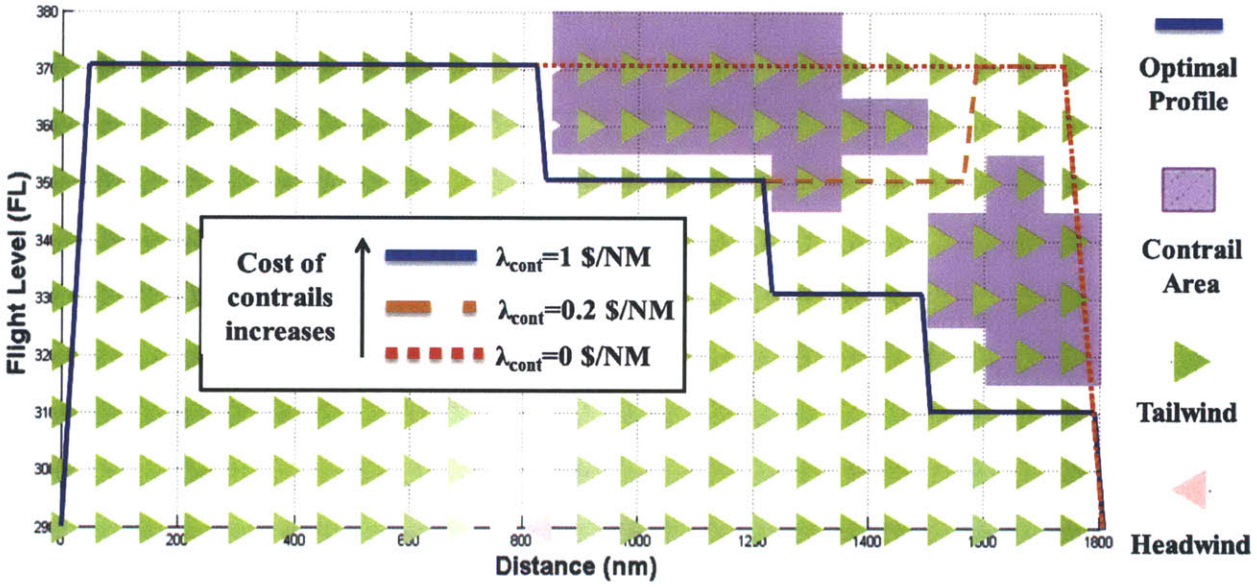

Figure 21 Example flight profile showing the impact of increasing the cost of contrails on the optimal flight profile. The weather shown is July 1, 2009 for LAX-JFK flying an A320. The flight profile is for instructional purposes only and is not actual results from the system model.

Furthermore, depending on the contrail density of the day, contrails may be unavoidable i.e. first days of January through April 2009. From Figure 22 it is observed that at a certain price of contrail per nautical mile (i.e. 0.6$/NM for A320) the contrail-minimal profile becomes the operating cost optimal. This is the contrail tax price at which the Pareto efficiency of contrail avoidance is reached: below this price point the profile still flies through avoidable contrail regions and above this point the contrail tax is overpriced with no additional gains in terms of avoidance. Therefore, while the ratio of avoidable to unavoidable is very variable to the weather day, an overarching trend suggests that such a price cap exists.

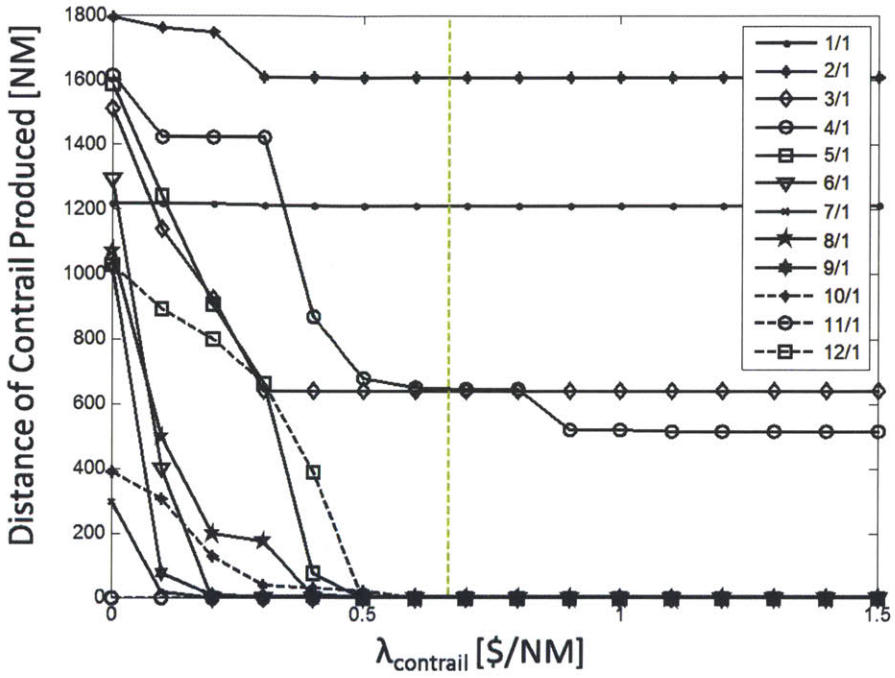

Figure 22 Sensitivity of contrail avoidance to weather conditions for A320. As the price of contrail per nautical miles increase, the optimal profile flown avoids more contrail producing regions. By 0.6$/NM the contrail minimal profile is found for most conditions.

To better visualize this price cap, the average distance through contrails for all 12 days were summed and plotted against the contrail valuation, λ_{cont}. As essentially the de-cluttered version of Figure 22, Pareto efficiency point is more clearly shown. Often referred to as the "knee" of the graph, this cost-efficient point designates the contrail valuation beyond which the relative cost is no longer worth the corresponding decrease in contrail production. There are a variety of methods that were developed in dealing with identifying these cost-benefit tradeoff points; for this analysis a simple geometric method will be used. This approach is done by deriving the slope of the line in Figure 23. The slope of line is the marginal contrail reduction per dollar increase of the contrail valuation. As the cost of contrail production increases near 0.6 dollar per nautical mile, there are virtually no additional contrails to avoid. Thus we have arrived at the price cap of contrail avoidance for the A320 for the 12 weather days.

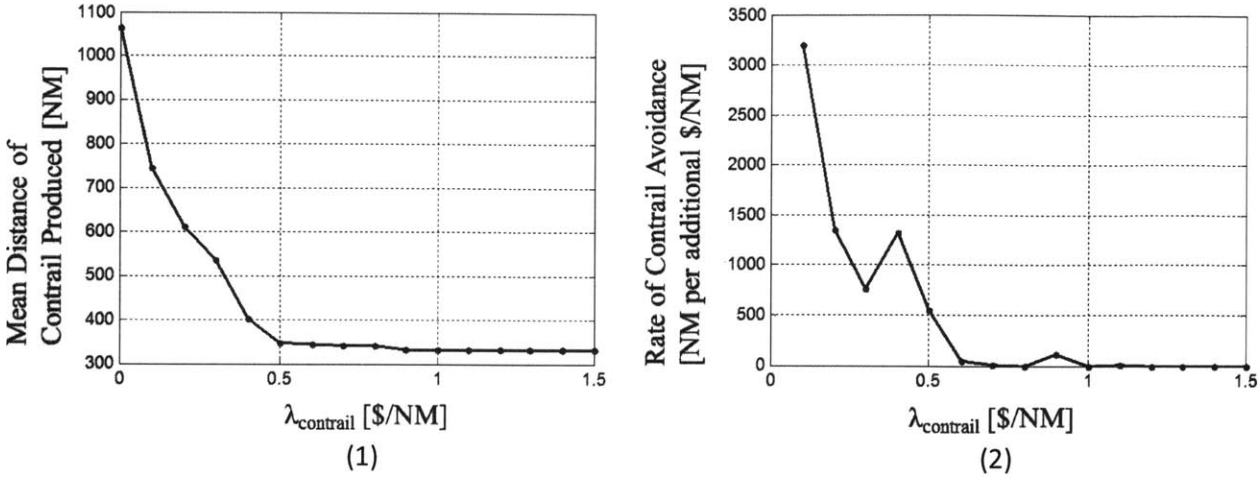

Figure 23 (1) The mean distance of contrail produced for all 12 days by flying the A320. At around 0.6 $/NM a clear cost-benefit tradeoff occurs and beyond which point the marginal contrail avoidance per marginal dollar of contrail is negligible. (2) Using the slope of (1), this plot shows the marginal contrail reduction per $/NM increase. The "knee" of the graph is identified as the point where the rate of contrail avoidance reaches 0. At this point the additional increase in the contrail valuation results in no additional contrail avoidance, which is roughly 0.6 $/NM for the A320.

4.2 Aircraft Sensitivity

From Piano-X, aircraft performance data for 11 aircraft types are extracted for this analysis (Table 2). The goal is to determine whether the cost to avoid contrails vary greatly with the type of aircraft flown. Each aircraft is characterized by their performance and block operating cost. Larger aircraft will tend to have higher block operating cost due to higher crew, maintenance, and aircraft costs. Compared to smaller aircraft, larger aircraft will also require more fuel to make the same avoidance maneuver and thus induce more emissions. Therefore it is expected that that long-haul aircraft such as the A330-200 and the B777-300ER will require a higher price of contrail to achieve the same contrail avoidance as small aircraft like the A320. In fact, this expectation holds true as shown in Figure 25. Interesting, aside from the atypical long-haul aircraft types, the majority of aircraft types had a price cap around 0.6 $/NM. The four lines distinctly to the right of the others represent the heavies: B777-300ER, A330-200, B767-300ER, and B767-200ER. The magnitude by which each of these long-haul carriers differed from the main pack is directly proportional to the size of the aircraft, i.e. the B777-300ER is the heaviest of the 11 and also has the highest "knee" point around 0.9$/NM.

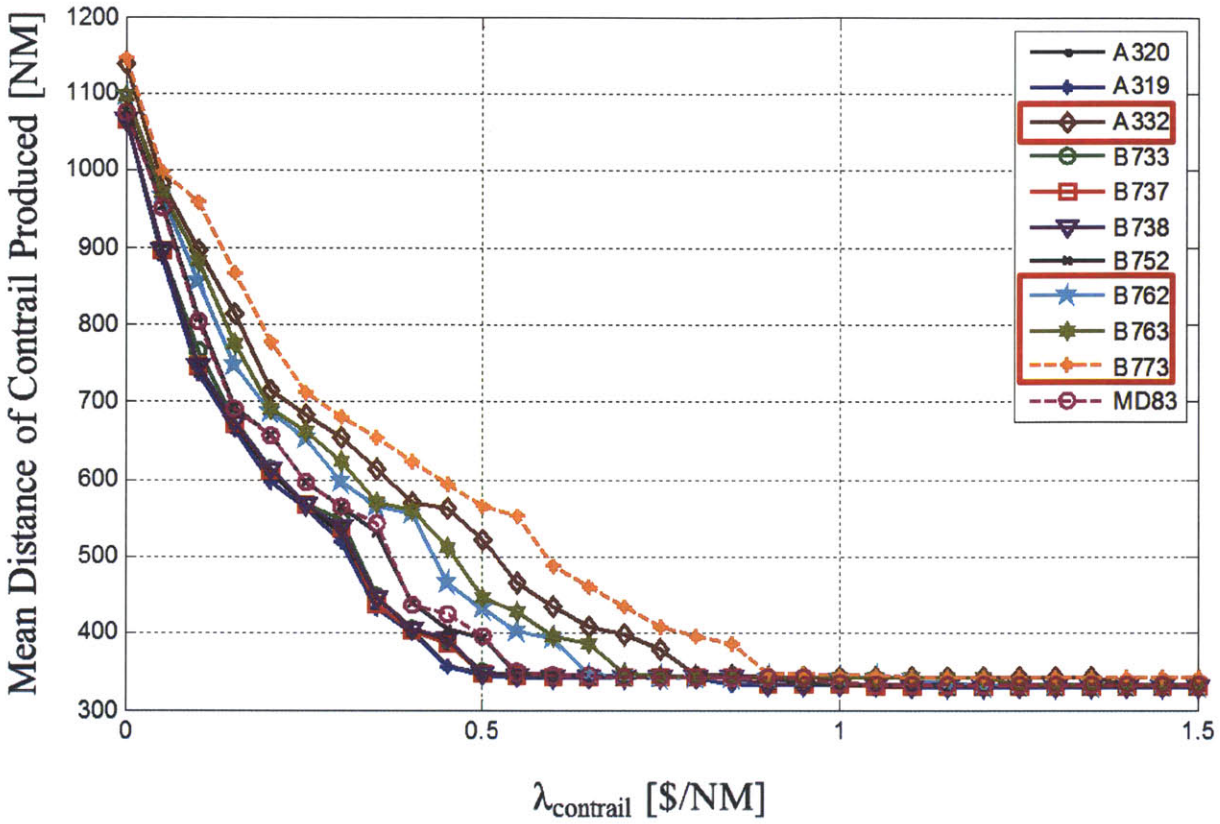

Figure 24 The mean distance of contrail produced for the 12 weather days for all 11 aircraft types. The heavies are outlined in red. While the "knee" of each aircraft differs, the general trends are similar and appear to be scalable by contrail valuation.

Another trend to note is that at 0$/NM cost on contrail production, the mean distance through contrail regions differ slightly by aircraft type. In fact, the B777-300ER and A330-200 are flying through more contrail regions than the smaller, short-haul aircraft types. The reason is due to the difference in the optimal cruise altitude that different aircraft are designed for. Aircraft such as the B777-300ER are designed to flight at higher altitudes, which shows especially for a long trip such as LAX-JFK. Had it been a shorter trip, the heavies would not have lost enough weight through fuel burn to step climb to the higher cruise altitudes. By flying through higher altitudes, the aircraft goes through denser contrail forming regions and incurs more contrail production.

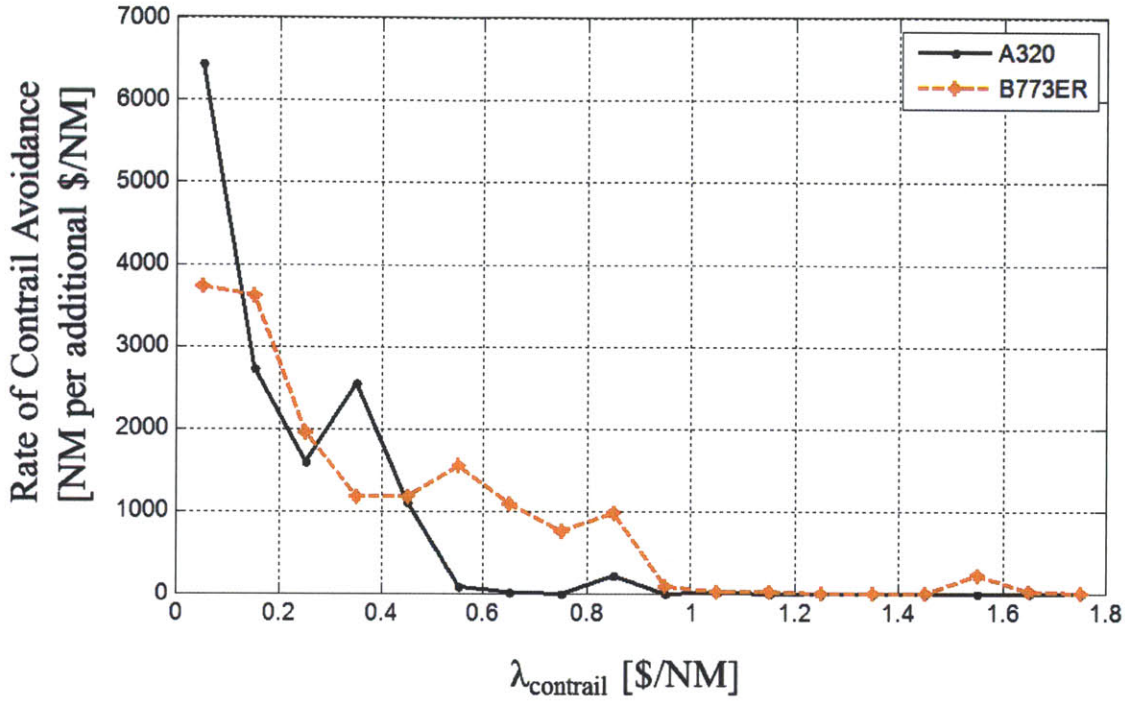

Figure 25 The rate of contrail avoidance per additional $/NM for all 11 aircraft types. The trends of the two aircraft types are similar, but the price caps appear at different contrail valuations. i.e. The slight bump in the rate of contrail avoidance at 0.85 $/NM for the A320 shows up at 1.5 $/NM for the B777-300ER.

As the contrail valuation is increase, heavies tend to avoid contrails at a slower rate than the medium-sized aircraft types. By, once again, plotting the rate of contrail avoidance per marginal contrail valuation increase comparing the A320 and B777-300ER, it is observed that the B777-300ER trends similarly to the A320 but is scaled to a higher price cap (Figure 25). This scaling difference holds true for other aircraft types as well. This observation suggest that while difference aircraft types cannot agree on one price cap, the scalability of the contrail avoidance behavior for different aircraft can be used to derive a normalized price cap, specific to certain aircraft characteristics.

4.3 Price Cap

From the weather and aircraft sensitivity analysis, the price cap has already been introduced as the maximum cost-effective contrail tax. Above this price cap, the contrail tax is overpriced and has no additional gain in contrail avoidance. First we will take a look at the price cap mentioned earlier. After that we will explore the cost tradeoff between contrail avoidance and the additional

fuelburn. From this a lower bound of contrail tax is derived to complement the price cap and complete the derivation of a price range for contrail tax.

To recall, the price cap is the contrail valuation point when contrail avoidance becomes the cost-optimal strategy to fly and beyond which point no significant contrail reduction is observed. Before any further discussion on deriving the operating price cap of contrail avoidance, let's briefly look at the purpose behind finding the operating price cap. Interest in reducing anthropogenic climate impact has existed long before contrails, extending even before the advent of aviation. From an economics perspective, global warming activities such as emissions are labeled as negative externalities, which are products that have negative effects beyond the producer and consumer. A common method in dealing with these negative externalities is by internalizing the negative effect by way of a Pigouvian tax. Through taxation on the product, the producer and consumer are effectively paying for the external effects, meanwhile also reducing the amount of production. The tax is found by estimating the social cost of the product and then internalizing the social cost into the cost of production. While currently no estimates on the social cost have been established for contrail production, the operating cost to avoid it becomes important. The contrail producers, which are the jet-engine aircraft operators, must be incentivized to pay the tax by referencing the cost of the taxation to the cost to perform the contrail avoidance. Since from an operator's perspective, the two options are to ignore contrail production or to avoid contrail producing regions. The price cap, therefore, is the minimum cost to operationally avoid contrail producing regions by flight level changes. Note that if, instead of taxation, the regulatory approach to control contrail production is cap and trade, where individual operators are allotted certain distance of contrail production, then operators may choose to fly contrail avoiding flight plans for smaller aircraft types given their lower price cap.

An advantage of the scalability of contrail avoidance by contrail valuation for different aircraft types is that a normalized contrail valuation can be derived such that the price cap is customized to each aircraft type, characterized by their size. A common measure of size used, i.e. in land fees, is the maximum takeoff weight (MTOW) of the aircraft.

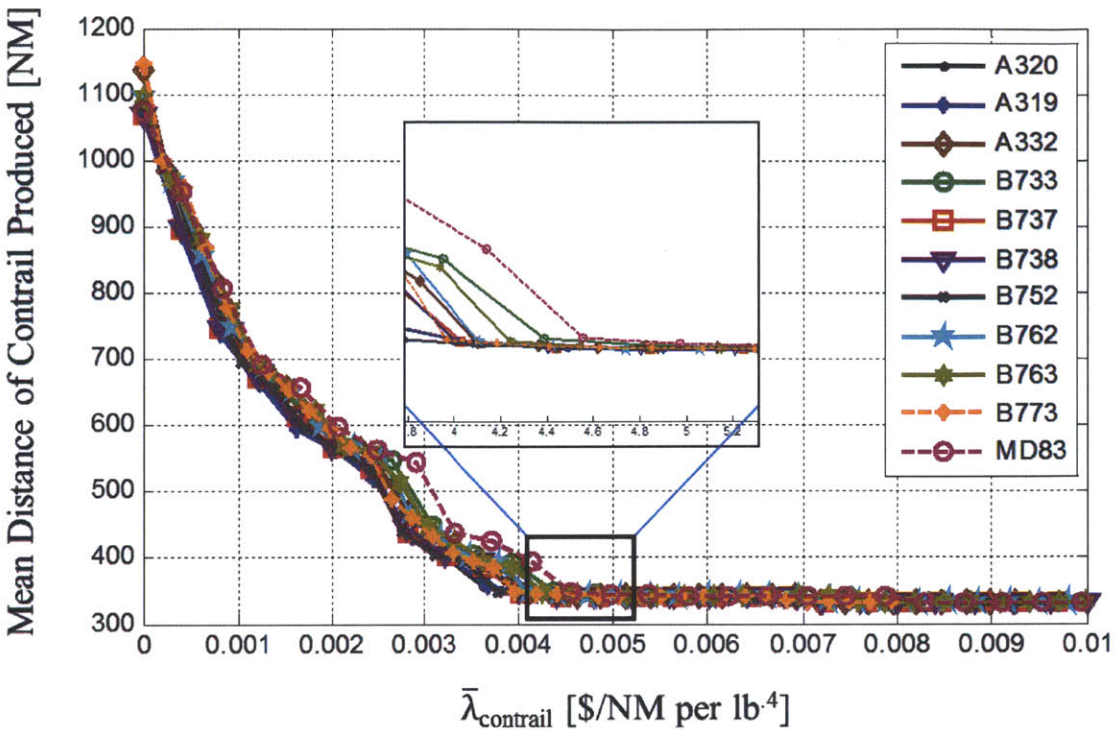

Figure 26 Normalized sensitivity plot shows a generalizable price cap at 0.0045 $/NM per lb. Note that the MD83 is a slight outlier, possibly due to the aging technology's relatively poor fuel economy that drives up the fuel cost.

Here the contrail valuation, $\lambda_{contrail}$, is normalizing by the MTOW$^{0.4}$, where the power of 0.4 is purely for fitting purposes. Using the normalized $\lambda_{contrail}$, the price cap for contrail avoidance can be derived by the following equation:

$$\lambda_{contrail} = \bar{\lambda}_{contrail} \cdot MTOW^{0.4}$$

Where $\bar{\lambda}_{contrail}$ is 0.005 $/NM by observing the "knee" of the plot in Figure 26. Using this method, the price cap of contrail avoidance for different aircraft types can be easily backed out based on the aircraft MTOW.

Table 7 Derived price cap for 11 aircraft types.

	B737-300	B737-700	B737-800	MD83	A319	A320	B757-200	B767-200ER	B767-300ER	A330-200	B777-300ER
Price Cap ($/NM)	0.569	0.588	0.588	0.603	0.612	0.618	0.727	0.866	0.880	0.966	1.134

4.4 Fuelburn Tradeoff

The price cap is the tradeoff point of contrail avoidance when considering the total cost of all tradeoff variables. Another important tradeoff point is between contrail avoidance and the additional fuelburn. This looks to see at what contrail tax cost is the additional fuel cost worth the contrail avoidance. Here we will set the baseline as when $\lambda_{contrail}$ equals to 0 \$/NM. The baseline scenario will traverse through a certain distance of contrail forming regions, which is the baseline distance of contrail produced. When we adjust for higher $\lambda_{contrail}$, the distance of contrail produced should decrease from the baseline and the difference is the distance of contrail avoided. To avoid these contrail regions, the aircraft had to burn additional fuel. Therefore, from the baseline fuelburn, any additional fuelburn will be the considered the fuel used in avoiding contrail production. By evaluating the marginal price of the avoided contrails to the marginal cost of the additional fuelburn used, the relative tradeoffs between the two variables are. Results show that the tradeoff between contrail avoidance and fuelburn favors contrail avoidance when the contrail valuation nears the price cap, but is too fuel cost intensive at lower contrail valuations (Figure 27).

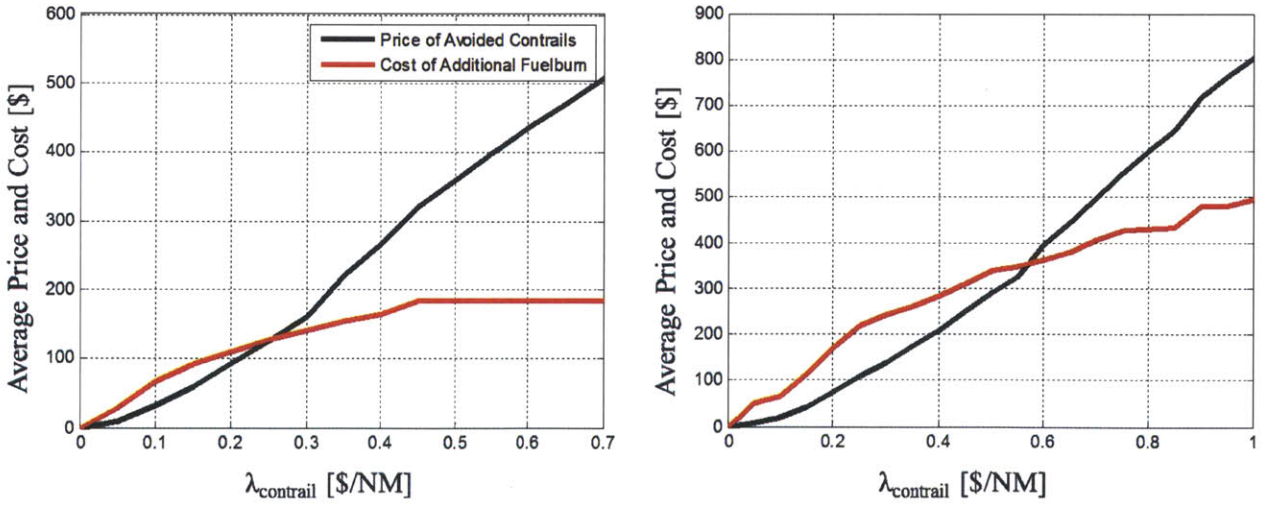

Figure 27 The cost tradeoff between the price of the contrail avoided and the cost of the additional fuelburn for the A320 (left) and the B77-300ER (right) using the current jet fuel cost of 3\$/gal. The crossing between the price of contrails and the cost of fuelburn is the **fuelburn tradeoff point**. Note that at the price cap of the A320 of 0.7\$/NM the monetary value of contrail avoidance outweighs the fuelburn needed to perform the avoidance strategy; similarly for the B777-300ER at 1\$/NM.

This suggest that a contrail tax ranging from 0.25 to 0.6 $/NM for the A320 is worth the fuelburn necessary to perform the avoidance strategy. The fuelburn tradeoff point varies for different aircraft types. In general, the larger the aircraft the higher the fuelburn tradeoff point (Figure 28). This may be due to the aircraft size and the aircraft's fuel efficiency. This fuelburn tradeoff point provides a minimum cost that contrails should have for contrail avoidance to be worth the additional fuel cost.

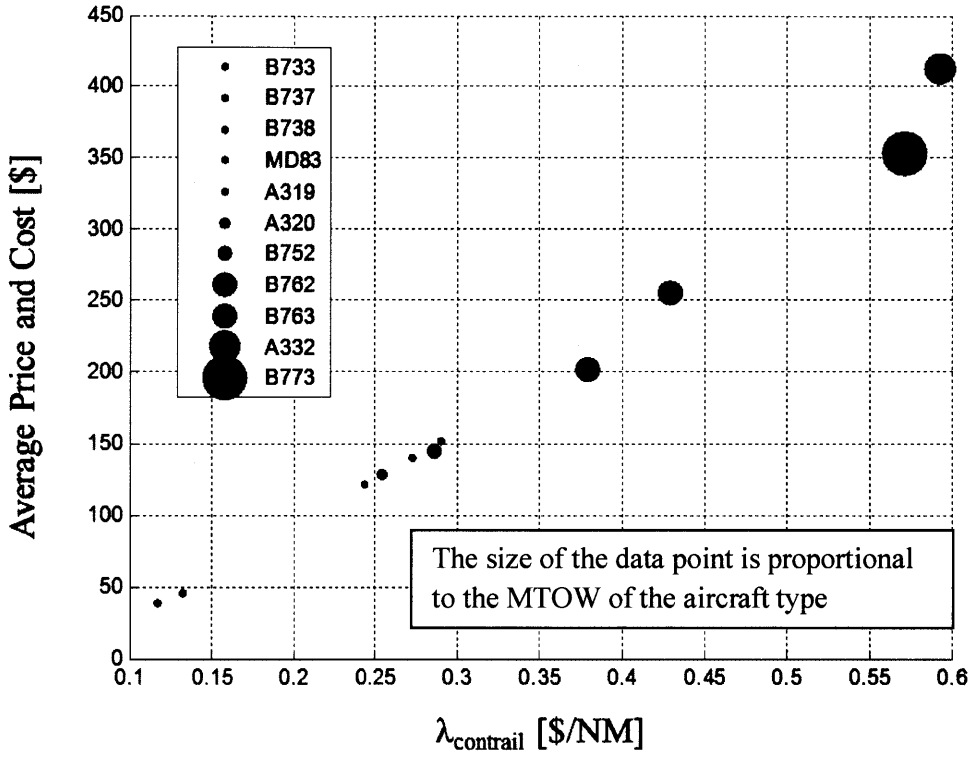

Figure 28 Fuelburn tradeoff points ($\lambda_{contrail}$ where the average price of contrail equals the cost of fuelburn) for 11 aircraft types with marker size scaled by respective MTOW. Beyond this point the cost of additional fuelburn is worth the price of contrail produced.

4.5 Summary of Contrail Tax Impact Study

Using the cost-based system model, the contrail tax impact study examined how a hypothetical cost on contrails effect the choice of the cost-optimal flight profile flown. By trading off the cost of contrails with the total operating cost (fuelburn, flight time, and emissions), a maximum cost-effective price cap is derived. The price cap is the maximum contrail valuation point where contrail avoidance is still the cost-optimal strategy to fly and beyond which point no significant contrail reduction is observed. This value is useful in providing a reference as to how much a contrail tax should cost for contrail avoidance to be worth the additional operating cost.

Additionally, a simplistic normalization method was introduced to derive the contrail tax price cap for different aircraft types based on their respective maximum takeoff weight. Similar to the method of deriving landing fees at airports, the contrail tax may require differentiating between aircraft due to the different operating cost needed for contrail avoidance. This study also determined a fuelburn tradeoff point, which is the minimum contrail valuation point where contrail avoidance is the cost-optimal strategy to fly and below which the cost of the additional fuelburn is higher than the savings in contrail avoidance. The fuelburn tradeoff point provides a lower bound of how much the contrail tax should cost. The results of this study are generalizable to 12 distinct weather days and 11 distinct aircraft types through the sensitivity analysis.

Chapter 5 – Climate Impact Study

This study looks to understand the climate impact of contrail avoidance strategies, assuming a contrail tax incentivizes such operations. First, this study will quantify the climate impact of the flight level optimization strategy, implemented on great circle, wind optimal, and AGTP optimal lateral routes. The great circle route is the shortest way for a given O-D and is useful as a baseline track to fly. The wind optimal route is the most fuel efficient way and is commonly used in current operations, making it another useful track to fly as reference. The wind optimal and AGTP optimal lateral routes are provided by a collaborating research team at NASA Ames. Once the climate impact of the flight level optimization strategy is explored, the strategy is then compared against the AGTP optimal lateral routes to determine the relative fuel efficiency of the two strategies at avoiding contrail production. Fuel efficiency here means the ratio between contrail avoidance and the additional fuelburn required. To account for the uncertainty in the latest contrail RF estimates, a range of values (3.3, 10, 30 mWm^{-2}) is used for this study. Furthermore, strategies optimized at different time horizon of climate impact are evaluated for their energy efficiency to determine whether it is more advantageous to design for a long-term climate impact objective or a short-term one. Based on the results of this study, recommendations are made on which contrail avoidance strategies should be used to minimize climate impact.

A total of 287 flights flying 12 O-D pairs throughout the day of April 12, 2010 were used in this study (Table 8). These selected flights use 7 distinct aircraft types (shaded in Table 2). The design of the 287 flights came from Federal Aviation Administration's assessment studies on the impact of Reduced Vertical Separation Minima (RVSM) strategies on aircraft fuelburn and emissions. For each of the 287 flights, all three types of lateral tracks are obtained and the flight level optimization is implemented.

Table 8 The 12 city pairs used in the climate impact study.

O-D Pairs	
Atlanta Hartsfield-Jackson (ATL)	Denver (DEN)
Dallas-Fort Worth (DFW)	Detroit Metropolitan (DTW)
Dallas-Fort Worth (DFW)	Washington Dulles (IAD)
Dallas-Fort Worth (DFW)	New York LaGuardia (LGA)
Detroit Metropolitan (DTW)	Minneapolis St. Paul (MSP)
Newark Liberty (EWR)	Houston George Bush (IAH)
Newark Liberty (EWR)	Miami (MIA)
Washington Dulles (IAD)	Orlando International (MCO)
Houston George Bush (IAH)	Phoenix Sky Harbor (PHX)
John F. Kennedy (JFK)	Los Angeles (LAX)
Chicago O'Hare (ORD)	New York LaGuardia (LGA)
Chicago O'Hare (ORD)	Miami (MIA)

5.1 Impact of Flight Level Optimization

To evaluate the effectiveness of contrail avoidance strategies, we have to compare the net AGTP ($AGTP_{contrail} + AGTP_{fuelburn}$) with that of baseline flights that flew without flight level changes. Therefore, for each of great circle and wind optimal lateral tracks, the AGTP-based vertical optimizer was implemented for the 287 flights and the net AGTP is evaluated. Additionally, by flying the AGTP lateral optimal tracks provided by NASA Ames, an additional comparison can be made between the vertical and lateral optimization strategies. Therefore a total of three baseline lateral tracks are used in this analysis (Figure 30)

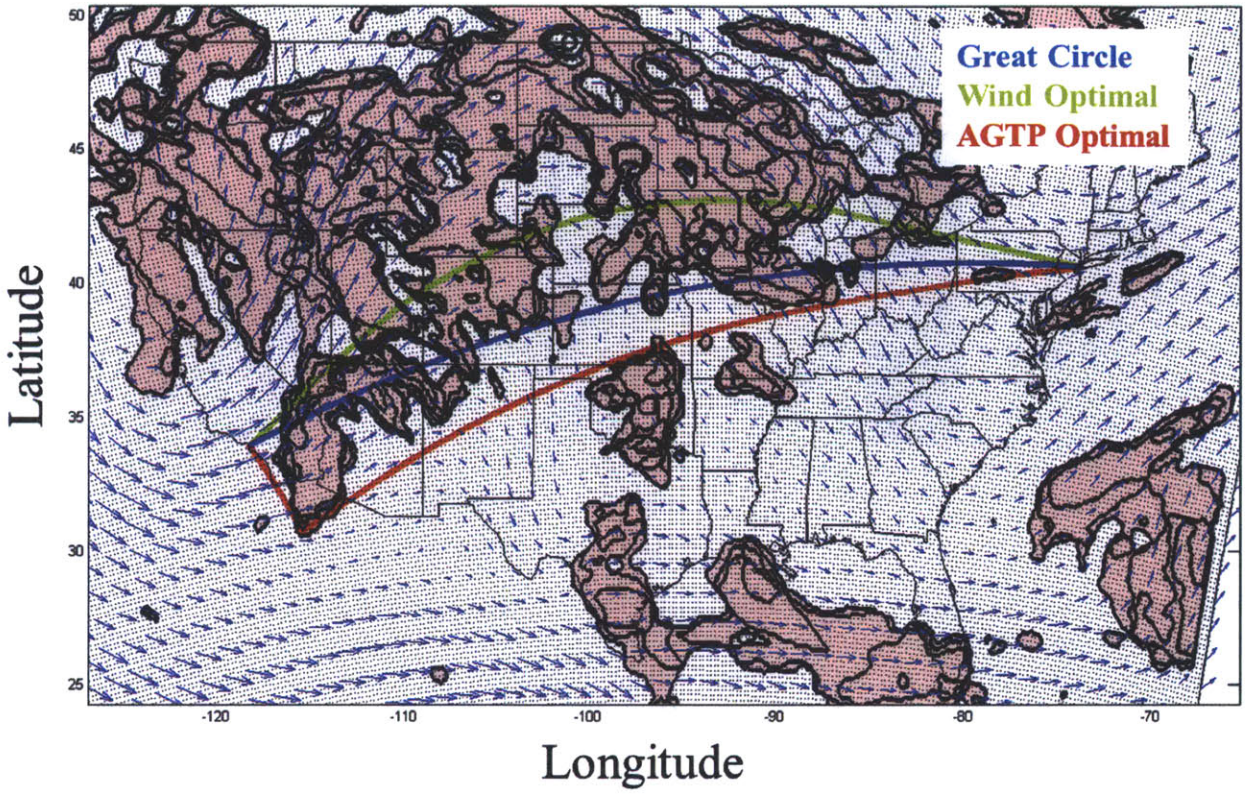

Figure 29 Representative lateral track types for LAX-JFK at 8UTC flown with an A320. The contrail producing region from FL290-FL410 is shown in magenta. The quivers indicate the wind vector at the optimal cruise altitude of FL350. The great circle, wind optimal and AGTP optimal lateral tracks are shown in blue, green and red lines respectively.

First, the results show a consistent reduction to the average AGTP per flight from the baseline scenarios by implementing the vertical optimizer. The reduction is greater for great circle and wind optimal lateral tracks than with the laterally optimized track (Figure 30). This, as we will see later, is due to the inherent fuel efficiency of great circle and wind optimal tracks. The AGTP lateral optimal tracks generate excess AGTP from fuelburn of the lateral deviations to avoid contrail producing regions, which in the following study is proven to be less fuel efficient than by vertical optimization using flight level changes. By implementing a lateral optimizer first followed by a vertical optimizer, the resulting flight plan does not take advantage of the fuel efficiency of vertical contrail avoidance and instead deviates to a suboptimal lateral track that is less fuel efficient. This result is consistent with all contrail RF assumptions and time horizon of evaluation. This result shows that flight level optimization indeed reduces the climate impact of the cruise phase by flight level adjustments. Furthermore, the reduction appears greater for great circle and wind optimal tracks than AGTP optimal lateral tracks.

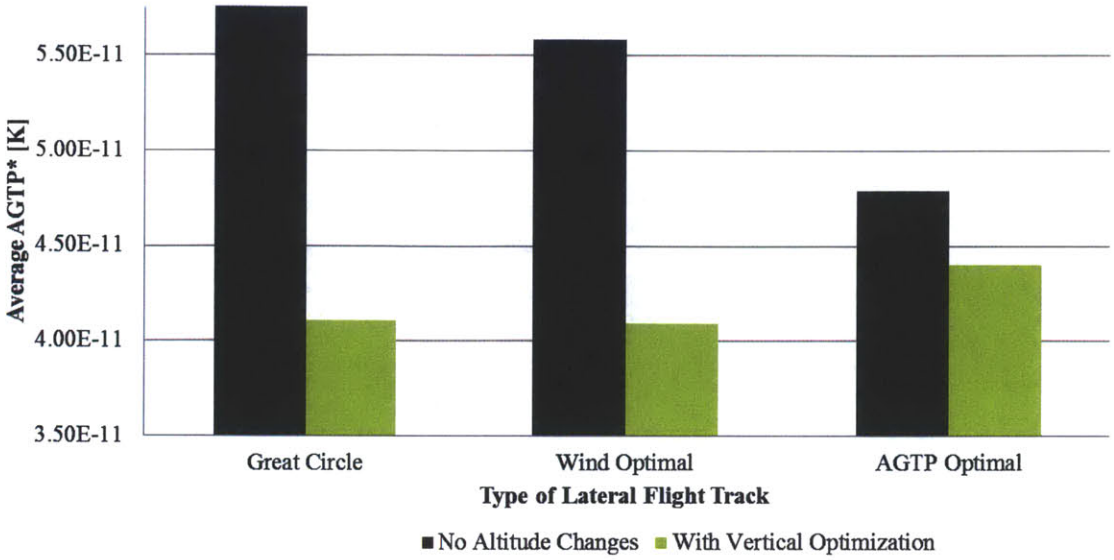

Figure 30 Vertical AGTP optimization implemented for three types of lateral tracks and all consistently show reduction in the average net AGTP ($AGTP_{contrail}$ + $AGTP_{fuelburn}$) contributed per flight. This plot is specific to contrail RF of 30 mWm^{-2} and time horizon of 25 years. The trend is consistent for all values of contrail RF and time horizon (See Appendix B).

To quantify the percentage of reduction by flying the different strategies, the wind optimal track with no flight level changes is set as baseline; we compared the laterally optimal, vertically optimal, and lateral plus vertical optimal strategies. The results suggest that vertically optimizing for AGTP sees the greatest reduction. Therefore if the intent is to minimize the climate impact of a flight, contrail avoidance should be done by making flight level changes.

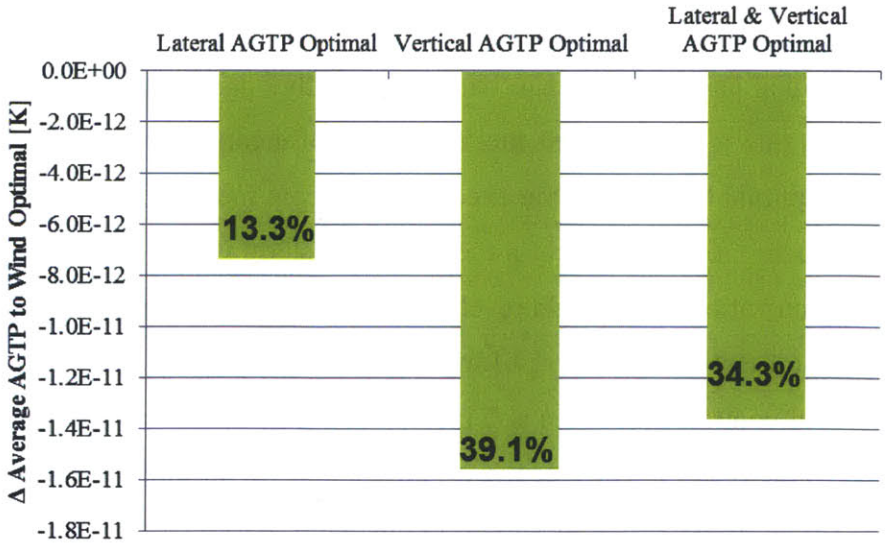

Figure 31 The average net AGTP reduction of various operational strategies using wind optimal lateral track as the baseline. This plot is specific to contrail RF of 30 mWm^{-2} and time horizon of 25 years. The trend is consistent for all values of contrail RF and time horizon.

So far, we have established that vertical AGTP optimization performs better at reducing the average net AGTP than other strategies such as lateral or lateral & vertical optimization. However this tells us little regarding the amount of additional fuelburn that is required to fly these strategies. Therefore next we will investigate how much fuel was consumed for each strategy. The efficiency of these strategies can be evaluated by breaking up the net AGTP value into the $AGTP_{contrail}$ reduction and the $AGTP_{fuelburn}$ addition.

5.2 Fuel Efficiency Comparison

The goal of this analysis is to identify whether vertical or lateral optimization is more fuel efficient in contrail avoidance. Recalling back to the way contrails evolve as discussed in Chapter 1, the growth rate is greater laterally than vertically. We allude to that contrail regions are geometrically flat and widespread. Furthermore, contrail formation is dictated by relative humidity, making it dependent on the ambient temperature. Since the atmospheric temperature is relatively homogenous for a pressure altitude, contrails are more likely to span a layer of the atmosphere than a range of pressure altitudes. These observations subsequently suggest that vertical contrail avoidance is easier than lateral maneuvering and possibly has an advantage in fuel efficiency. To test this hypothesis, the 287 flights were flown using the wind optimal track as the baseline reference. Then at different contrail RF, the AGTP-optimal vertical and lateral optimizations were run as comparison to the wind optimal baseline. The climate impacts of these strategies are evaluated at time horizons of 25, 50, and 100 years. The net AGTP is used to quantify the climate impact of each strategy and the total fuel consumption is used to quantify the fuel efficiency of each strategy. Results suggest that flight level optimization is able to reduce the climate impact by a greater amount at the cost of less fuelburn compared to using lateral optimization (Figure 32). Furthermore, the overall climate impact diminishes at longer time horizons due to radiative forcing decay.

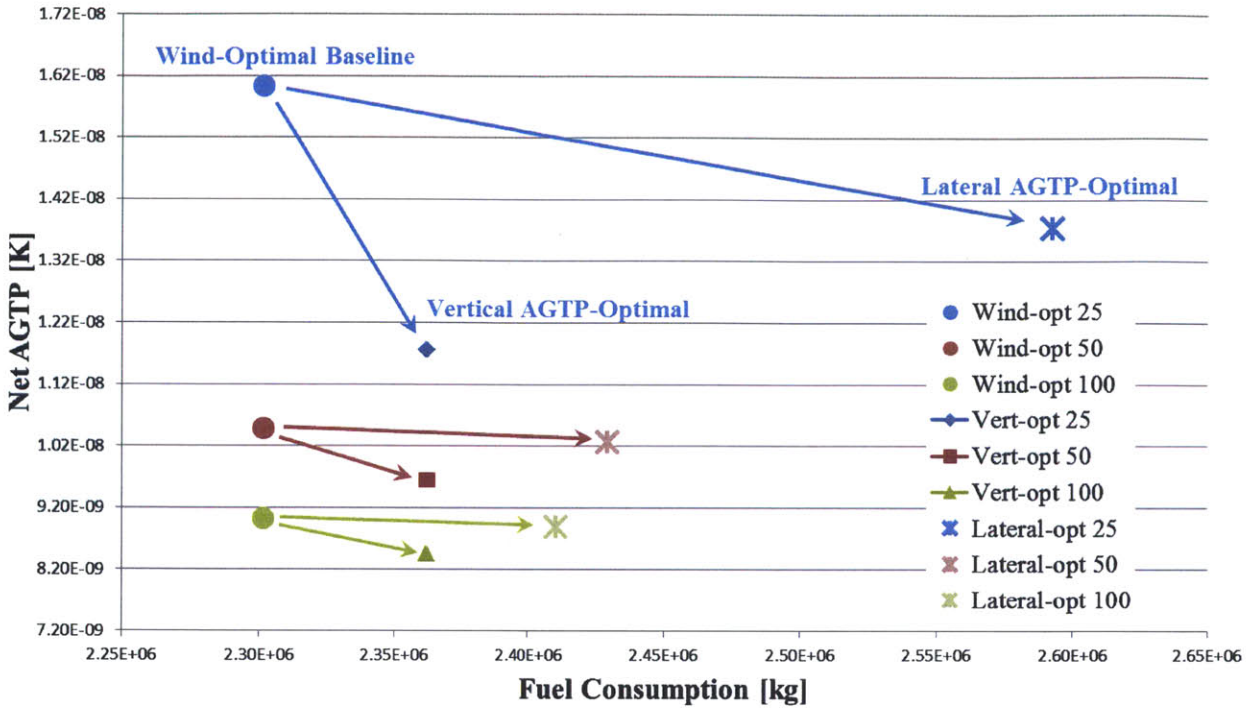

Figure 32 Comparison between the climate impact reduction and fuel efficiency of vertical and lateral AGTP optimization strategies for contrail RF of $30mWm^{-2}$. The time horizon of climate impact is shown in blue (25 years), red (50 years), and green (100 years).

The climate impact of the additional fuel consumption used in contrail avoidance was also compared to the baseline wind optimal case (Figure 33.a). The climate impact incurred by the lateral strategy is almost 4 times that of the vertical strategy. Whereas the vertical strategy reduced the climate impact of contrails by over 90% compared to 60% using lateral. Another observation worth mentioning is that, instead of using additional fuelburn to avoid contrails, a reduction in fuelburn was observed at low contrail RF and long time horizon (Figure 33.b). The reason behind this behavior is that vertical optimizer is able to fly a more fuel optimal flight profile by changing from the optimal cruise altitude depending on the wind conditions. At long time horizons, the impact of contrail becomes negligible due to their short lifetime. On the other hand, CO_2 emission has long lasting climate impact and becomes a more significant part of the net radiative forcing. Therefore, with low contrail RF and less impactful time horizons, contrail avoidance becomes less important and the AGTP optimal profile more and more resemble the wind optimal profile.

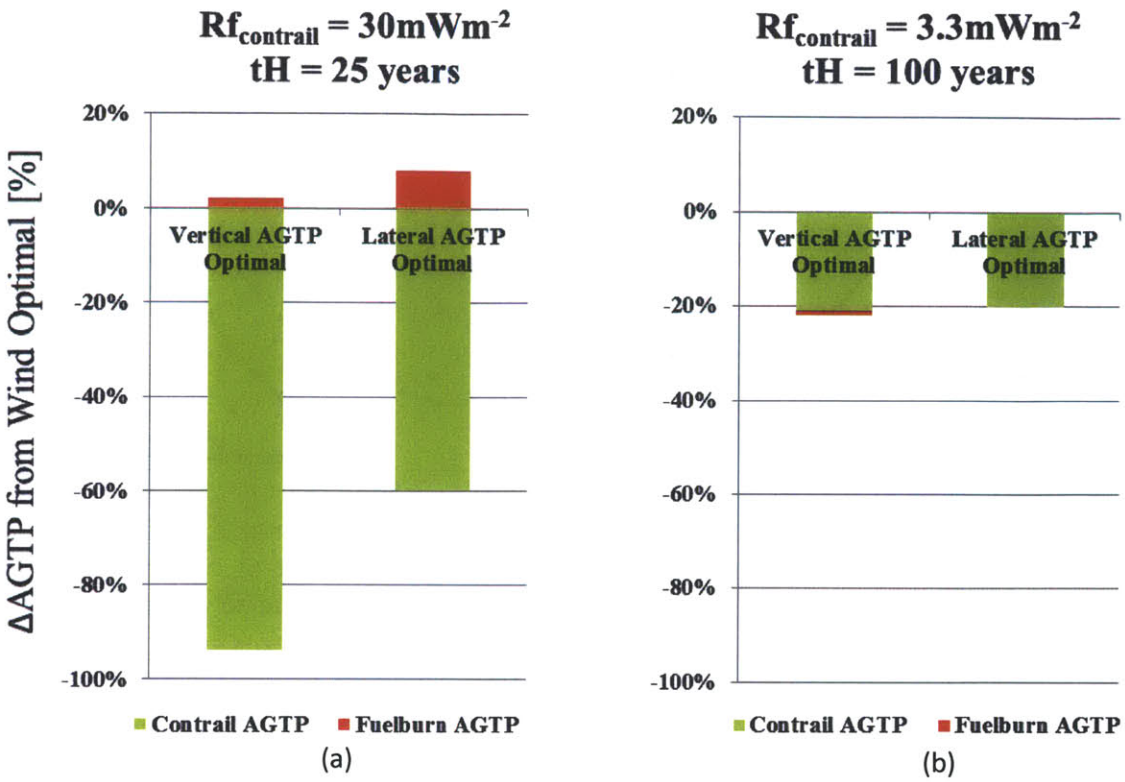

Figure 33 (a) Wind optimal lateral track and fixed optimal cruise altitude as baseline, the percentage increase in the AGTP due to fuelburn is less for vertically optimized flights than laterally optimized ones. This is consistent for all $RF_{contrail}$ and time horizon assumptions. (b) Note that at low contrail RF and long time horizon, vertical optimization are able to fly a more wind optimal profile by adjusting flight levels based on wind conditions and thus reducing the AGTP due to fuelburn. More results tabulated in Appendix C.

To verify the relative importance of AGTP due to fuelburn at lower contrail RF and longer time horizons, a sensitivity analysis was conducted on the tradeoff between contrail and fuelburn. The findings conclude that as the climate impact of contrail diminishes with lower RF assumptions and longer time horizon, the impact of additional fuelburn eventually outweighs the benefit of contrail avoidance (Figure 34). This suggests that at low contrail RF estimates, contrail avoidance is not climate optimal due to the overwhelming additional emission that results from these strategies.

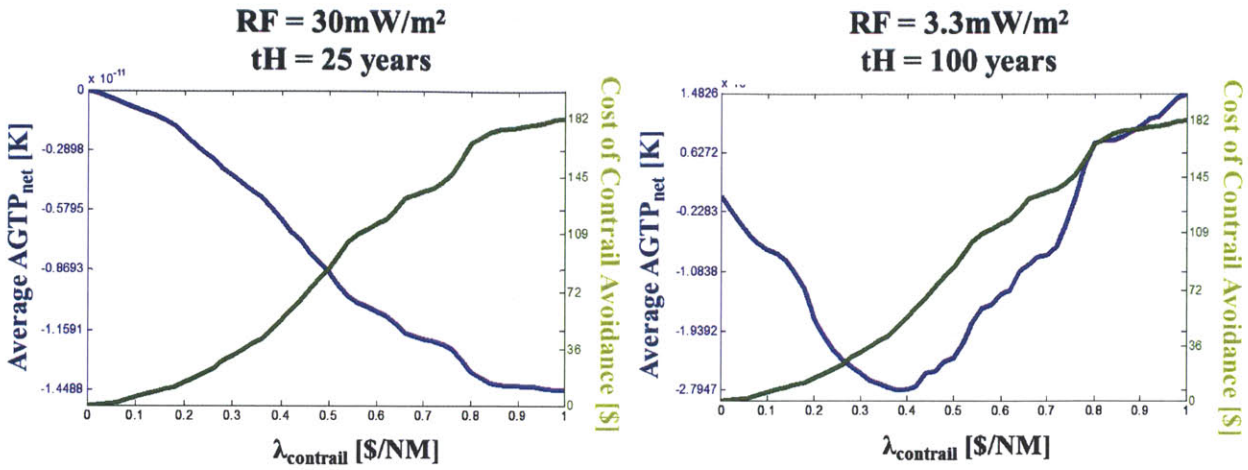

Figure 34 Sensitivity of AGTP at different contrail RF assumptions and climate impact time horizons generated using the cost-based system model. As the cost of contrail increases, the $AGTP_{fuelburn}$ eventually outweigh that due to contrail formations due to the difference in the lifetime of these two climate impact factors.

5.3 Energy Efficiency of Climate Optimal Strategies

So far in this study, AGTP optimal strategies are designed for a specific time horizon and their climate impacts are evaluated at the same time horizon. It is interesting to investigate whether it is more advantageous to design for one time horizon over another. In other words, is there one time horizon that climate impact optimal strategy should be designed at? To answer this question, flight level optimization was used to design climate impact optimal strategies at the end of 25, 50, and 100 years and the strategies are subsequently evaluated at the end of all three time horizons i.e. a contrail avoidance strategy AGTP optimized at the end of 25 years is evaluated at the end of 50 and 100 years. To evaluate the effectiveness of these strategies, the energy efficiency metric is used. Energy efficiency is a measure of the effectiveness of the contrail avoidance strategy in terms of AGTP reduction per unit of additional fuelburn.

$$Energy\ Efficiency = \frac{AGTP\ reduction\ [K]}{Additional\ fuelburn\ [kg]}$$

The results show that the optimal strategy that minimizes total climate impact at the end of 100 years appears to have the highest energy efficiency compared to optimizing for 25 and 50 years (Figure 35). Note also that the energy efficiency of a strategy is higher when the time horizon being evaluated is shorter. This is indicative of contrail's short term climate impact. While the contrail RF is impactful at short time frames, the climate impact decays as the time

scale extends. Therefore when the climate impact is evaluated at a longer time scale, the AGTP reduction from contrail avoidance diminishes. This trend holds true for all three contrail radiative forcing assumptions.

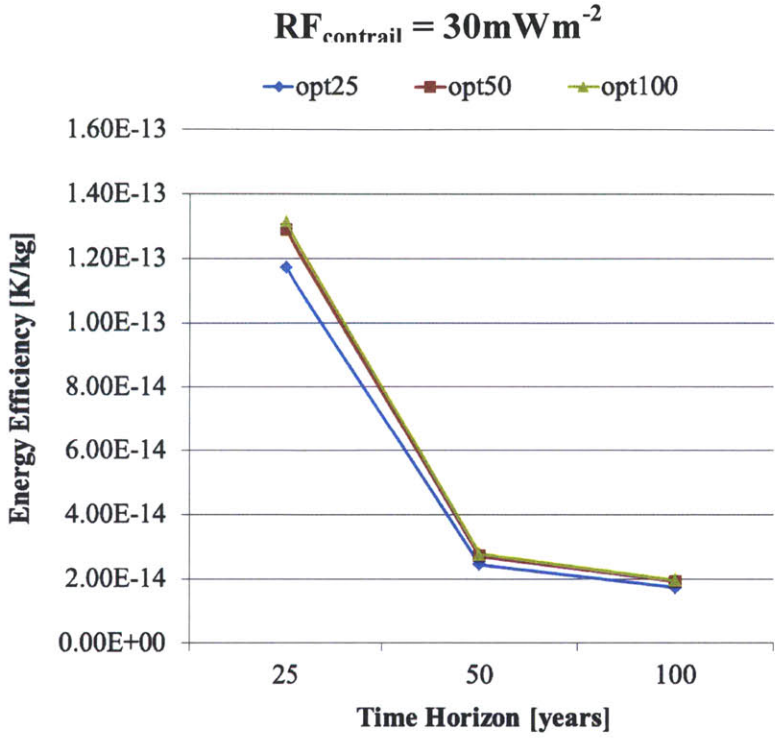

Figure 35 The energy efficiency at $30mWm^{-2}$ for strategies designed to be climate optimal for 25 (blue), 50 (red), and 100 (green) years. The time horizon at which the climate impact is evaluated is shown on the x-axis. See Appendix D for more results.

5.4 Summary of Climate Impact Study

Using the AGTP-based system model, the climate impact study examined and compared various contrail avoidance strategies using 287 flights. Starting with the flight level optimization, or vertical optimization, the strategy offers an average climate impact reduction of 39.1% from the wind optimal baseline, assuming the contrail RF is $30mWm^{-2}$. Furthermore, this strategy proves to be more effective than lateral optimization by allowing more climate impact reduction while consuming less fuel. This study has also found that designing the AGTP-optimal strategy at a time horizon of 100 years is more energy efficient than at 25, or 50. This suggests that a long-term environmental objective is preferred when fuel consumption is considered alongside climate impact reduction through contrail avoidance.

Chapter 6 - Conclusion

The results of this research investigated the effect of a hypothetical contrail tax on incentivize contrail avoidance from an operating cost perspective. Findings suggest that contrail tax may cap off at a certain point above which no additional benefit in contrail avoidance is possible. Furthermore, results suggest that the contrail tax has a price range dependent on the size of the aircraft. The climate impact of different operational contrail avoidance strategies is evaluated and recommendations are made regarding strategies that are more efficient in mitigating the climate impact from contrails and CO_2 emission. Result also suggests the time scale climate impact optimal flight profiles should be designed for using the energy efficiency metric that measure the climate impact reduction per additional kilogram of additional fuelburn.

6.1 Contrail Tax

Using the cost-based system model, the lower and upper bound of the price of contrail tax are explored for 11 different aircraft types using 12 different weather days. The fuelburn tradeoff point, the lower bound of the contrail tax, is the minimal price on contrails such that the cost of the additional fuelburn is less than the price of the contrails avoided in the optimal profile flown. Above this price, contrail avoidance is worth the cost of the additional fuel consumed. However, below this price, the tradeoff favors producing the lower cost contrails to fly more fuel efficiently.

The price cap, the upper bound of the contrail tax, denotes the lowest cost of contrails that results in maximum achievable contrail avoidance. The marginal gain in the additional distance of contrails avoided becomes negligible beyond this price point. From a policy point of view, the social cost of contrails should be above the fuelburn tradeoff point for aircraft operators to consider altitude-based contrail avoidance, which indicates contrail avoidance is worth the cost of additional fuelburn. The price cap of the contrail tax gives a preliminary reference point to the operating cost of contrail avoidance, above which point no additional significant benefit in contrail avoidance is observed. Since operating cost for contrail avoidance differs depending on the type of aircraft use, the price range derived in this study is dependent on the aircraft of interest. A normalization method is introduced to derive the price range depending on the maximum takeoff weight (MTOW) of the aircraft. MTOW is a simple characteristic to distinguish different aircraft types for taxation and is often used in aviation taxes such as landing fees at airports. Assuming that contrail avoidance is incentivized, result shows that smaller aircraft of the fleet require a lower contrail tax to execute contrail avoidance and are preferred to heavies.

6.2 Climate Impact

Climate impact is measured for a given time horizon using the AGTP metric. This climate impact metric measures the global temperature change at the end of a time scale (25, 50, 100 years for this research) contributed by the radiative forcing agent being evaluated. Assuming aircraft operators are incentivized to fly contrail minimal strategies, results show that flight level optimization is more efficient than lateral optimization. By making flight level adjustments to avoid contrail forming regions, the aircraft burn less fuel and produces a lower distance of contrails for 287 flights encompassing 12 O-D pairs, a 24 hour weather day, and 7 aircraft types. For example, using the contrail RF of 30 mWm^{-2} and evaluation at the end of 25 years, the flight level optimization reduced 94% of the climate impact due to contrail from the baseline case of wind-optimal at cruise optimal altitude with no flight level change. In contrast, lateral optimization reduced 60% of the climate impact from the same baseline case. In terms of fuelburn, lateral optimization used 4 times the additional fuel for contrail avoidance compared to flight level optimization. From this, it appears that the climate impact optimal strategy is to fly a wind-optimal lateral track and use flight level optimization to minimize climate impact.

Since climate impact is dependent on the time scale of the measurement, climate impact optimal strategies differ depending on the time horizon of the intended design. Result shows that long-term designs are more energy efficient, which is the measure of the climate impact reduction per kilogram of additional fuel consumed. Since the climate impact of contrails is short-term (on the order of decades) compared to that of CO_2 (over a century), this result suggests that the most effective strategy values minimizing CO_2 emission to contrail avoidance. Therefore the energy efficiency analysis suggests that the climate impact optimal strategy to fly is closer to a fuel minimal profile than a contrail avoidance strategy, based on the current climate impact estimates of contrails and CO_2 emissions.

Bibliography

(IPCC), I. P. (1999). *Aviation and the Global Atmosphere.*

Airbus. (2012). *Global Market Forecast 2012-2031.*

Alduchov, O., & Eskridge, R. (1996). Improved Magnus Form Approximation of Saturaiton Vapor Pressure. *Journal of Applied Meteorology*, 601-609.

Burkhardt, U., & Karcher, B. (2011). Global Radiative Forcing From Contrail Cirrus. *Nature.*

Campbell, S. (2008). An Optimal Strategy for Persistent Contrail Avoidance. *Guidance, Navigation and Control* (p. 16). Honolulu: AIAA.

Degrand, J. Q., & Carleton, A. M. (1977-1979). A Satellite-Based Climate Description of Jet Aircraft Contrails and Associations with Atmospheric Conditions. *Journal of Applied Meteorology*, 1434-1459.

Gierens, K. (2008). A Review of Various Strategies for Contrail Avoidance. *The Open Atmospheric Science*, 1-7.

IPCC. (2012). *Chapter 8: Anthropogenic and Natural Radiative Forcing (Draft 2).* Not yet published.

IPCC WGI. (2012). *Chapter 8: Anthropogenic and Natural Radiative Forcing.* IPCC WGI.

Jager, H., Freudenthaler, V., & Homburg, F. (1998). Remote Sensing of Optical Depth of Aerosols and Clouds Related to Air Traffic. *Atmospheric Environment*, 3123-3127.

Jensen, E. J. (1998). Spreading and Growth of Contrails in a Sheared Environment. *Journal of Geophysical Research*, 31557-31567.

Kohler, M. O. (2008). Impact of Perturbations to Nitrogen Oxide Emissions From Global Aviation. *Journal of Geophysical Research.*

Myhre, G., & Stordal, F. (2001). On the Tradeoff of the Solar and Thermal Infrared Radiative Impact of Contrails. *Geophysical Research Letters*, 3119-3122.

Noppel, F. (2007). *Contrail and Cirrus Cloud Avoidance Technology.* Cranfield: Cranfield University.

O'Neill, G., & Hansman, R. (2012). *An Approach to Analyze Tradeoffs for Aerospace System Design and Operation.* Cambridge: Department of Aeronautics and Astronautics, MIT.

Peters, G. A. (2011). The Integrated Global Temperature Change Potential (iGTP) and Relationships Between Emission Metrics. *Environmental Research Letters.*

R. Meerkotter, U. S. (1999, December 14). Radiative Forcing by Contrails. *Annales Geophysicae*, pp. 1080-1094.

Reynolds, T., & Gillingwater, D. (2009). *Climate Related Air Traffic Management Final Report.* Loughborough: Loughborough's Institutional Repository.

Roberson, B. (2007). Fuel Conservation Strategies: Cost Index Explained. *Aero Quarterly*, 26-28.

Sausen, R. (2005). Aviation Radiative Forcing in 2000: An Update on IPCC (1999). *Meteorologische Zeitschrift*, 555-561.

Schrader, M. (1997). Calculations of Aircraft Contrail Formation Critical Temperatures. *American Meteorological Society*, 1725-1729.

Schumann, U. (2009). *A Contrail Cirrus Prediction Tool.* Cologne: DLR.

Sridhar. (2012). Integration of Linear Dynamic Emission and Climate Models with Air Traffic Simulations. *Guidance, Navigation, and Control* (p. 15). Minneapolis: AIAA.

Sridhar, B. C. (2011). Design of Aircraft Trajectories Based on Trade-offs Between Emission Sources. *9th USA/Europe ATM R&D Seminar* (p. 10). Berlin: ATM.

Yen, J. Y. (1971). Finding the K Shortest Loopless Paths in a Network. *Management Science*.

Appendix A

The full tradeoff solution space reduced to 3-dimensional space using principle component analysis for the LAX-JFK flight for the weather day February 1, 2009.

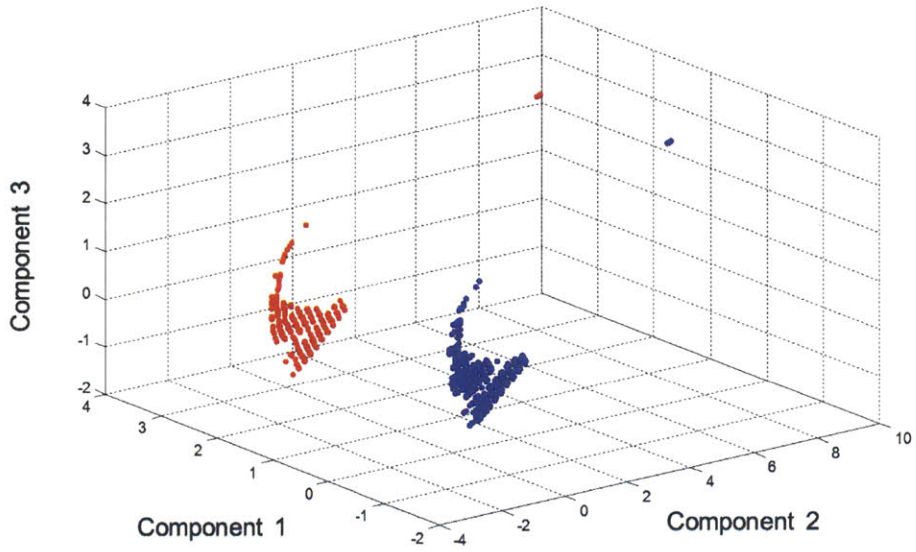

Figure 36 Clusters of 2/1/2009 LAX-JFK flight profile solution space reduced to 3 dimensions using PCA. The red cluster climbed from the initial ascent into cruise while the blue cluster leveled off at FL290 to avoid producing contrails at higher altitudes.

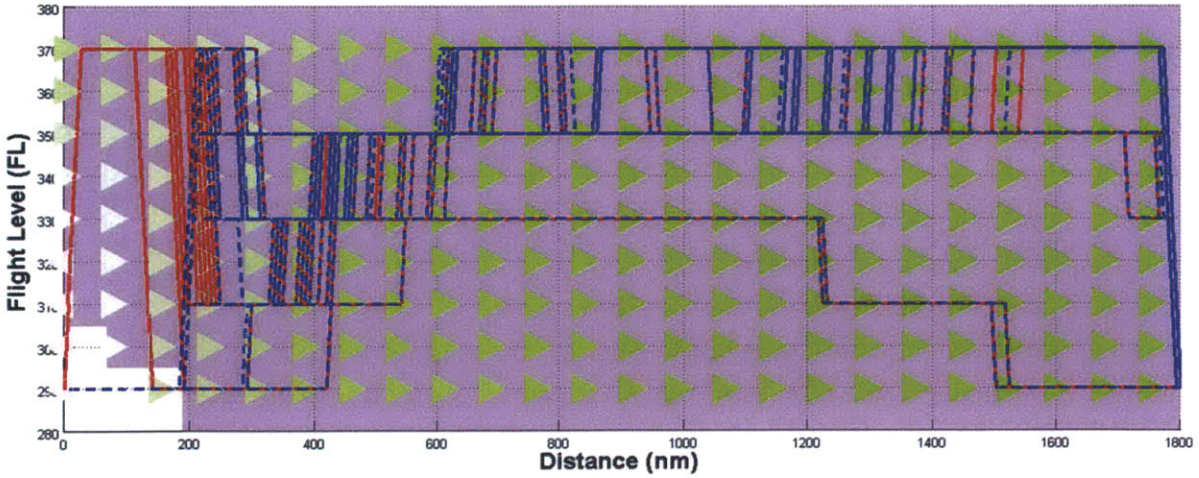

Figure 37 All flight profiles in the tradeoff solution space differentiated by the clusters in the previous figure.

Appendix B

Flight level optimization reduces the climate impact of great circle, wind optimal, and AGTP optimal flights for time horizons of 50 and 100 years.

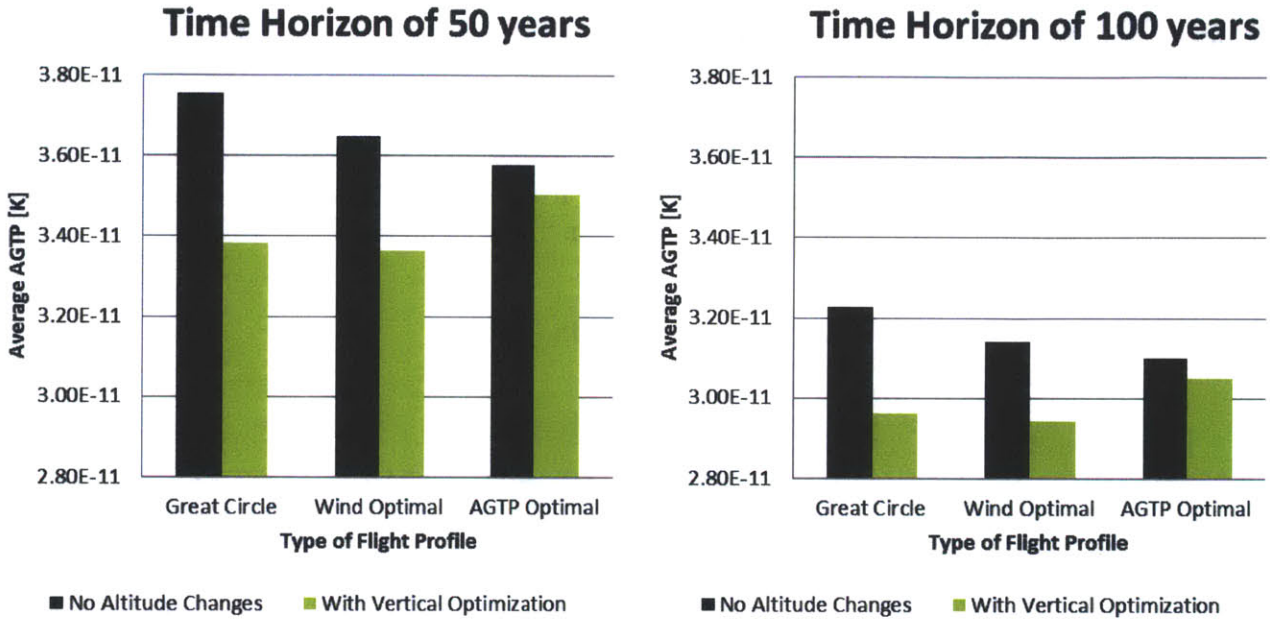

Figure 38 The reduction of average climate impact from the baseline wind optimal flight profile with a fixed cruise altitude by implementing flight level optimization.

Appendix C

Tabulated below is the climate impact reduction by contrail avoidance strategies (vertical and lateral) and the increase in the climate impact due to CO_2 emission from additional fuelburn; shown as percentage difference in AGTP from the wind optimal baseline flight under 9 different contrail radiative forcing and time horizon assumptions.

Table 9 For 3 different contrail radiative forcing assumptions and measured at the end of 3 different time horizons: (a) Percentage reduction of AGTP due to contrails from baseline wind-optimal flight profile with no flight level changes using vertical and lateral optimization. (b) Percentage increase in AGTP due to CO_2 emission from additional fuelburn for vertical and lateral optimization.

$AGTP_{contrail}$ reduction (%) by:

Vertical optimization

RF [W/m^2]	Time Horizon [yrs] 25	50	100
3.3	85%	28%	21%
10	94%	78%	69%
30	94%	93%	93%

Lateral optimization

RF [W/m^2]	Time Horizon [yrs] 25	50	100
3.3	43%	21%	20%
10	56%	41%	39%
30	60%	54%	51%

$AGTP_{fuelburn}$ addition (%) due to:

Vertical maneuvering

RF [W/m^2]	Time Horizon [yrs] 25	50	100
3.3	1%	-1%	-1%
10	1%	1%	0%
30	2%	1%	1%

Lateral maneuvering

RF [W/m^2]	Time Horizon [yrs] 25	50	100
3.3	2%	0%	0%
10	6%	2%	2%
30	8%	5%	4%

Appendix D

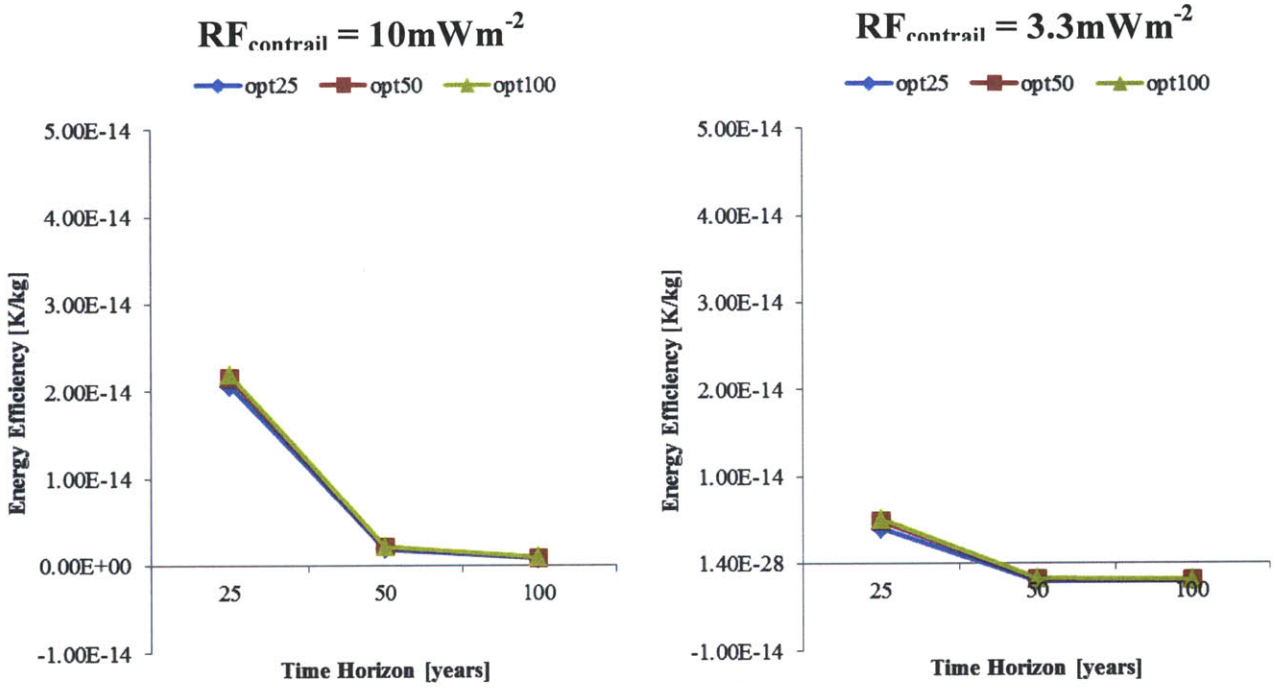

Figure 39 The energy efficiency of climate impact optimal strategies designed for different time horizons; contrail radiative forcing assumptions of 10 and 3.3mWm^{-2}. The efficiency drops as the benefit of contrail avoidance is diminished with the lower contrail RF.